First publ. in: Journal of Comparative Neurology ; 499 (2006), 6. - pp. 933-952

Dual Olfactory Pathway in the Honeybee, *Apis mellifera*

SEBASTIAN KIRSCHNER,[1] CHRISTOPH JOHANNES KLEINEIDAM,[1] CHRISTINA ZUBE,[1] JÜRGEN RYBAK,[2] BERND GRÜNEWALD,[2] AND WOLFGANG RÖSSLER[1]*

[1]Department of Behavioral Physiology and Sociobiology, Biozentrum, University of Würzburg, Würzburg, Germany

[2]Institut für Biologie, Neurobiologie, Freie Universität Berlin, Berlin, Germany

ABSTRACT

The antennal lobes (ALs) are the primary olfactory centers in the insect brain. In the AL of the honeybee, olfactory glomeruli receive input via four antennal sensory tracts (T1–4). Axons of projection neurons (PNs) leave the AL via several antenno-cerebral tracts (ACTs). To assign the input–output connectivity of all glomeruli, we investigated the spatial relationship of the antennal tracts and two prominent AL output tracts (medial and lateral ACT) mainly formed by uniglomerular (u) PNs using fluorescent tracing, confocal microscopy, and 3D analyses. Furthermore, we investigated the projections of all ACTs in higher olfactory centers, the mushroom-bodies (MB) and lateral horn (LH). The results revealed a clear segregation of glomeruli into two AL hemispheres specifically supplied by PNs of the medial and lateral ACT. PNs of the lateral ACT innervate glomeruli in the ventral-rostral AL and primarily receive input from T1 (plus a few glomeruli from T2 and T3). PNs of the medial ACT innervate glomeruli in the dorsal-caudal hemisphere, and mainly receive input from T3 (plus a few glomeruli from T2 and T4). The PNs of the m- and l-ACT terminate in different areas of the MB calyx and LH and remain largely segregated. Tracing of three mediolateral (ml) ACTs mainly formed by multiglomerular PNs revealed terminals in distinct compartments of the LH and in three olfactory foci within the lateral protocerebrum. The results indicate that olfactory input in the honeybee is processed via two separate, mainly uPN pathways to the MB calyx and LH and several pathways to the lateral protocerebrum.

Indexing terms: antennal lobe; olfactory glomeruli; 3D-reconstruction; projection neurons; mushroom bodies; lateral horn; antenno-cerebral tract

Recognition of a large variety of odors is crucial for many animals, which probably was a major driving force for convergent evolution of common design principles in primary olfactory centers in such diverse taxa as insects and mammals (Hildebrand and Shepherd, 1997; Strausfeld and Hildebrand, 1999). Odor molecules are received by olfactory receptor neurons (ORNs) dispersed in sensory epithelia, and ORN axons project to primary olfactory centers, the vertebrate olfactory bulb (OB) or the insect antennal lobe (AL). The synaptic neuropil of the OB and AL is compartmentalized in spheroidal neuropil units, so-called olfactory glomeruli (e.g., reviewed by Anton and Homberg, 1999; Christensen and White, 2000). Axons of ORNs expressing the same odorant receptor or with similar odor specificities converge on individual glomeruli and are relayed to projection or output neurons (PNs) (e.g., Hildebrand and Shepherd, 1997; Hansson and Christensen, 1999; Rössler et al., 1999; Galizia and Menzel, 2000; Vosshall et al., 2000; Xu et al., 2000; Carlsson et al., 2002; Wang et al., 2003). Consequently, glomeruli can be regarded as functional units for odor processing, and glomerular arrays constitute a chemotopic sensory map. In

This article includes Supplementary Material available via the Internet at http://www.interscience.wiley.com/jpages/0021-9967/suppmat.

Grant sponsor: German Science Foundation DFG; Grant number: SFB 554 (A6) and (A8); Grant sponsor: University of Würzburg.

*Correspondence to: Wolfgang Rössler, Department of Behavioral Physiology and Sociobiology, Zoology II, Biozentrum, University of Würzburg, Am Hubland, 97074 Würzburg, Germany.
E-mail: roessler@biozentrum.uni-wuerzburg.de

most olfactory systems the input–output relationship within these spatial maps of olfactory glomeruli is still poorly understood, and it is unclear whether a spatial organization is conserved in higher olfactory centers. In the present study we address these issues in the well-established olfactory pathway of the honeybee.

The relatively small number and species-specific anatomical arrangement of glomeruli in the honeybee AL allowed individual identification of many glomeruli and detailed 3D analyses of glomerular maps (Arnold et al., 1985; Flanagan and Mercer, 1989; Galizia et al., 1999b). The antennal nerve (AN) splits into six sensory tracts upon entrance to the AL. Four of these tracts (T1–T4) innervate distinct clusters of glomeruli in the AL, the two remaining tracts (T5, T6) bypass the AL and project to the antennal mechanosensory center in the deutocerebrum (called the dorsal lobe, DL), the subesophageal ganglion (SOG), and the caudal protocerebrum (Pareto, 1972; Suzuki, 1975; Mobbs, 1982; Galizia et al., 1999b; Abel et al., 2001). A recent study demonstrated that axons of the multiple (5–35) ORNs of single pore–plate sensilla (the predominant type of olfactory sensilla in the honeybee) enter the AL via all four sensory tracts (T1–4), and each ORN innervates a different glomerulus (Kelber et al., 2006). This indicates that olfactory input from multiple ORNs of individual pore–plate sensilla is dispersed onto glomeruli throughout the AL.

It is not known whether the four sensory tracts (T1–T4) in the honeybee separate the corresponding glomeruli into functional groups or clusters of glomeruli. Several calcium-imaging studies in the honeybee AL describe odor response profiles of individual glomeruli (Joerges et al., 1997; Galizia et al., 1999a; Sachse and Galizia, 2003). These optical recording techniques give good access only to glomeruli in the upper half of the AL, which are supplied mainly by sensory tract T1. Thus, so far calcium-imaging studies do not provide data on whether the tract-specific clusters of glomeruli in the honeybee AL represent any functional units of, e.g., different odor qualities or odor categories.

At least five antenno-cerebral tracts (ACTs) leave the honeybee AL toward higher centers of the brain, including the mushroom bodies (MBs) and the lateral horn (LH) (Mobbs, 1982; Abel et al., 2001). The medial and lateral output tracts (m- and l-ACT) are most prominent, containing primarily axons of uniglomerular projection neurons (uPNs) that target both the MBs and LH (Bicker et al., 1993; Abel et al., 2001; Müller et al., 2002; Brandt et al., 2005). In addition, at least three smaller ACTs, the mediolateral ACTs (ml-ACTs), contain mainly axons of multiglomerular projection neurons (mPNs) and project to the LH only (Fonta et al., 1993).

Intracellular recordings from individual uPNs of the m- and l-ACTs revealed differences in their response latencies and tuning properties in response to odors (Müller et al., 2002; Menzel and Manz, 2005). Müller et al. (2002) hypothesized that odor information from the AL may be transmitted via two parallel uPN output pathways coding different properties of the odor stimulus. Abel et al. (2001) showed that uPNs of the m-ACT receive input from glomeruli in the upper hemisphere of the AL, whereas uPNs of the l-ACT receive input from glomeruli in the lower hemisphere of the AL. This anatomical division of the AL by two groups of uPNs innervating hemispherical subsets of glomeruli indicates that these neurons receive different sensory input and this may result in a dual olfactory pathway.

Axonal terminals of uPNs are synaptically relayed to MB-intrinsic neurons, the Kenyon cells (KCs). The MB calyces of the honeybee are anatomically and functionally subdivided into the basal ring, collar, and lip (Mobbs, 1982; Gronenberg, 2001; Strausfeld, 2002). The lip region and the inner half of the basal ring receive olfactory input, whereas the collar and outer half of the basal ring receive visual input (Gronenberg, 2001). Any further spatial organization of antennal lobe input beyond this general organization has not yet been verified, except for some differences in the terminal arborization pattern of individual AL PNs (Abel et al., 2001). The second major target area of both the m- and l-ACT uPNs is the LH. In addition to the uPN innervation, the LH receives input from mPNs via the ml-ACTs, which were shown to project to the lateral protocerebrum only (Fonta et al., 1993). Studies in *Drosophila* indicated some degree of compartmentalization of the LH according to PN arborization patterns (Marin et al., 2002; Wong et al., 2002; Tanaka et al., 2004). In the honeybee, the spatial organization of PN projections in the LH is unknown.

In the present study we applied various fluorescent tracing techniques and confocal microscopy combined with 3D reconstructions to fill several gaps of our present knowledge about the spatial neuronal organization along the central olfactory pathways in the honeybee brain. We addressed the following questions: 1) What is the input–output relationship of glomeruli innervated by the four (antennal) sensory tracts (T1–4) and the uPN output tracts m- and l-ACT? 2) What is the spatial organization of terminals from uPNs of the m- and l-ACT in the MB-calyx and the LH? 3) What are the projections and terminal arborizations from mPNs of the ml-ACTs in the lateral protocerebral lobe and the LH?

MATERIALS AND METHODS

Tissue preparation

Honeybee workers (*Apis mellifera carnica*, n = 89) were collected at the entrance of a hive at the departmental bee station (University of Würzburg), anesthetized at 4°C, and positioned in metal tubes. After the head and antennae were fixed with dental wax (Dentaurum KG, Ispringen, Germany), a window was cut into the frontal head capsule between the compound eyes. Under repeated rinsing with bee-ringer solution (37 mM NaCl, 2.7 mM KCl, 8 mM Na_2HPO_4, 1.4 mM KH_2PO_4, pH 7.2), glands and trachea were removed to access the brain.

Following tracer application (see below), animals were kept alive in a moist dark chamber for 3–5 hours. Pilot experiments showed that diffusion time was sufficient for both dextran tracers (see below). Meanwhile, ringer was replaced every 30 minutes. Subsequently, animals were anesthetized at 4°C, the heads were cut off, and the brains were dissected and fixed in 4% formaldehyde in phosphate-buffered saline (PBS, pH 7.2) for 24 hours at 7°C. Brains were fixed and then washed in PBS, dehydrated in an ascending series of ethanol (50%, 70%, 90%, 95%, and 3 × 100%, 10 minutes each step), cleared in methylsalicylate (Sigma-Aldrich Chemie, Steinheim, Germany), and embedded as whole-mounts in Permount (Fisher Scientific, Schwerte, Germany) using 0.5-mm

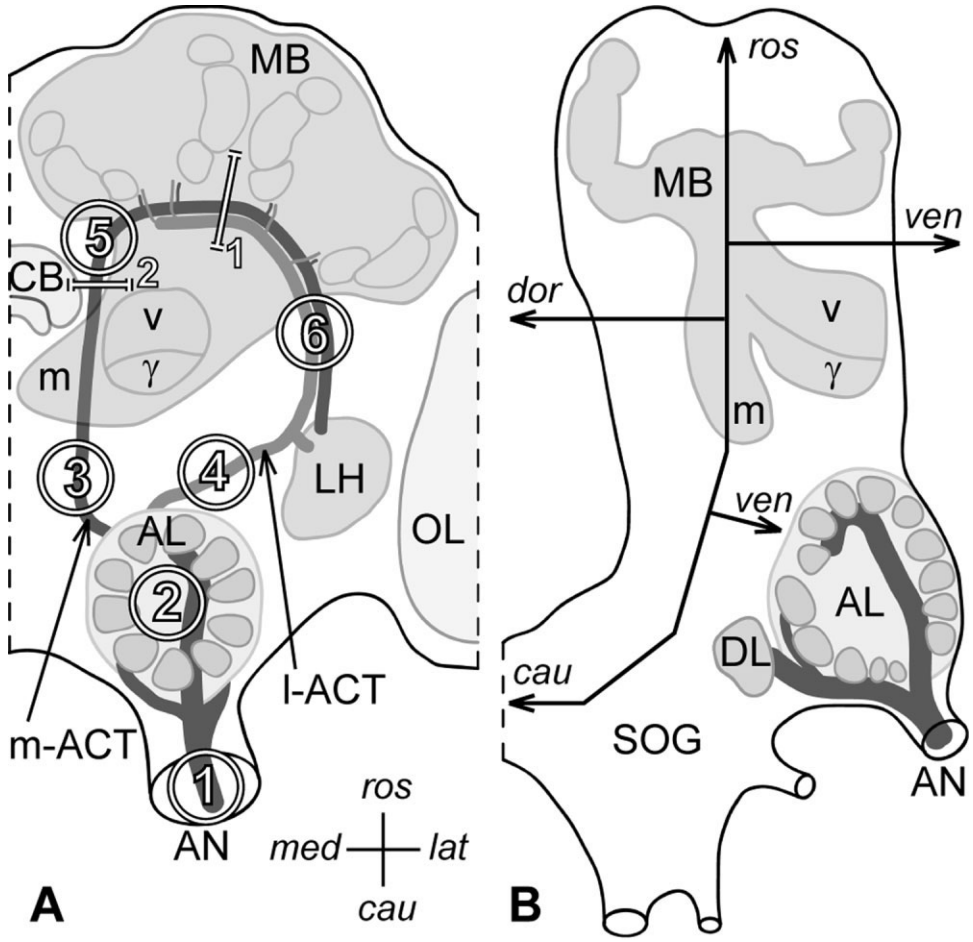

Fig. 1. Schematic drawing showing the different regions of tracer application (**A**) and anatomical directions of the honeybee brain (**B**). A: Vertical view. The circled numbers 1–6 indicate the locations for tracer application (see text for further details). Cuts 1 and 2 indicate regions that were severed to block dye diffusion via one of the two tracts depending on the staining procedure. B: Sagittal view showing the axis from caudal (cau) to rostral (ros) that causes the ventral side (ven) of the brain to appear upward in a vertical view and the dorsal side facing downward. AL, antennal lobe; DL dorsal lobe; AN, antennal nerve; SOG, subesophageal ganglion; CB, central body; LH, lateral horn; m- and l-ACT, medial and lateral antenno-cerebral tract; OL, optic lobes; MB, mushroom body with medial (m), vertical (v) and gamma (g) lobe.

thick aluminum slides with a central hole covered by thin cover slips from both sides. Whole-mounts were stored at −20°C.

Tracer application and immunohistochemistry

Depending on the AL output tract of interest, the tracer was applied at different locations in the deuto- and protocerebum (Fig. 1A). The different spatial directions used in this study refer to the neural axis of the honeybee's nervous system, which is bent about 90° backward at the level of the brain (Fig. 1B). Consequently, a vertical view as shown in Figure 1A reflects the ventral side of the brain to the point of view; the MBs appear rostral and the SOG caudal (Fig. 1B; nomenclature adapted after Strausfeld, 2002).

Fluorescent dextran conjugates were applied with the following procedure: glass electrodes were pulled with a horizontal puller (Sutter Instrument, Novato, CA). The brain tissue in the area of interest was carefully perforated with the tip of a glass electrode. Subsequently, the broken tip of a glass electrode was loaded with small dextran crystals (~200 μm in diameter) and used to transfer the tracer into the brain tissue. Two dextran conjugates were used: rhodamine dextran with biotin, 3,000 MW, lysine-fixable (Microruby, D 7162; Molecular Probes, Eugene, OR) and Alexa Fluor 488 dextran, 10,000 MW, lysine-fixable (D 22910; Molecular Probes). No obvious difference in the staining pattern using either dextran dye was found. The tracing electrode remained in the target tissue for several seconds to allow the dye crystals to dissolve and to be taken up by injured neurons. Immediately after withdrawal of the glass electrode the brain was rinsed with bee-ringer solution to reduce unspecific staining in the surrounding areas.

To identify AL glomeruli innervated by PNs that leave the AL via the medial or lateral ACT (m- and l-ACT), both tracts were retrogradely filled in single preparations, each with a different tracer. The m-ACT was labeled by tracer injection into the medial-rostral protocerebrum, where the

m-ACT curves around the peduncle of the MB (position 5 in Fig. 1A). The l-ACT was labeled by tracer injection into the lateral-rostral protocerebral lobe, at the position where the l-ACT proceeds from the MB toward the LH (position 6 in Fig. 1A). A sagittal cut was made between the two calyxes using a fine broken razor blade to separately label m- and l-ACT neurons in the AL (cut 1 in Fig. 1A).

For double labeling of the input and output of AL glomeruli via axonal projections of the ORNs and via the PNs of the m- or l-ACT, we combined anterograde labeling of the antennal nerve (AN) with a retrograde fill of either the m- or the l-ACT as described above. For the AN mass fill, the antenna was cut distally from the scapus and a crystal of dextran tracer was applied at the cut end (position 1 in Fig. 1A). For an overview of all connections of the AL with the protocerebrum, we applied the dextran tracer into the AL neuropil (position 2 in Fig. 1A).

To analyze the projection patterns of the m- and l-ACT within the MB calyces, we combined anterograde fills of the m- and l-ACT with different dextran conjugates in the same preparations. The m-ACT was labeled by dextran application into the medial-caudal protocerebrum, between the AL and medial lobe, at the position where the m-ACT exits the AL (position 3 in Fig. 1A). The l-ACT was labeled by dextran application into the lateral-caudal protocerebrum between AL and LH, at the position where the l-ACT exits the AL (position 4 in Fig. 1A).

Double staining of the m-ACT projections in the LH and those of the l-ACT, as well as ml-ACT 2 and 3, was achieved by combining anterograde mass fills of the m-ACT at the medial-rostral protocerebral lobe (position 5 in Fig. 1A) with a mass-fill of all other ACTs (including the l-ACT) via tracer injection into the AL (position 2 in Fig. 1A). To prevent tracer mixing in m-ACT neurons, a horizontal cut between the two MB calyces of one hemisphere was made before tracer application (cut 2 in Fig. 1A).

In one experiment, anti-synapsin immunohistochemistry was used as a marker for synaptic neuropil in the MB calyx (Fig. 6D,E). The primary antibody was a monoclonal antibody raised in mouse directed against the *Drosophila* synaptic vesicle-associated protein synapsin (SYNORF1; 3C11; kindly provided by E. Buchner, University of Würzburg, Germany), which was shown to recognize several synapsin isoforms in *Drososhila* brains (a protein triplet of 70, 74, and 80 kDa and a doublet at ~143 kDa; Klagges et al., 1996). In immunohistochemistry experiments in the honeybee and several other insect species, the antibody was shown to label synaptic neuropil in a very similar pattern as in *Drosophila* brains (e.g., Klagges et al., 1996; Frambach et al., 2004; Groh et al., 2004, 2006). Briefly, brains were immersed in cold 4% formaldehyde in PBS overnight at 4°C and then rinsed three times in PBS. Whole mounts were preincubated in PBS containing 0.2% Triton X-100 and 2% normal goat serum (NGS; ICN Biomedicals, Orsay, France, no. 191356) for 2 hours at room temperature and then incubated with the primary antibody (1:50; SYNORF1) for 3 days at 4°C in 500 μL PBST with 2% NGS. Preparations were subsequently rinsed in five changes of PBS, incubated in Alexa 488-conjugated goat antimouse secondary antibody (1:250; Molecular Probes, A-11001) in 1% NGS/PBS for 2 hours at room temperature, then processed as described above.

Confocal laser-scanning microscopy and image processing

For microscopic analyses, whole-mounts were viewed with a confocal laser-scanning microscope (Leica TCS SP; Leica Microsystems AG, Wetzlar, Germany) equipped with an argon/krypton laser. Scans were made by using two different oil HC PL APO objective lenses: UV 10x0.4NA (working distance 0.36 mm with oil immersion) or UV 20x0.7NA (working distance 0.25 mm with oil immersion). The excitation wavelength used for rhodamine was 568 nm and 488 nm for Alexa Fluor 488. Series of optical sections were captured at intervals of 1–10 μm, if necessary in combination with a 2–3× digital zoom. In doubly labeled preparations the two channels were scanned sequentially for each optical section.

Complete stacks of optical sections were imported in the 3D software Amira 3.1 (Mercury Computer Systems, Berlin, Germany), scaled, rotated around the z-axis, and cropped to the sector of interest. In doubly labeled preparations, for each channel a different false color was assigned (red for Microruby and green for Alexa 488) before combining both in one Amira image stack. In order to increase the signal-to-noise ratio, some data stacks were recomputed using a deconvolution (Amira 3.1). The data were viewed either as single orthoslices or as projection views of several consecutive orthoslices (see notes in figures).

Screenshots from slices or Amira reconstructions were further processed with Adobe Photoshop 7.0 software (Adobe Systems, San Jose, CA) and adjusted for brightness and contrast or served as templates for schematic drawings with Adobe Illustrator 10.0 software. For easier comparison, all orthoslices and projection views are shown in the vertical plane of the left half of the brain with the MB facing upward (rostral) and the SOG facing downward (caudal). Exceptions are indicated in the figures by coordinates. Abbreviations used for the different spatial directions are: rostral, r; caudal, c; ventral, v; dorsal, d; medial, m; and lateral, l (after Strausfeld, 2002). All scale bars are 100 μm.

3D reconstruction of antennal lobe glomeruli and neuronal tracts

In the published reconstructions of the honeybee AL (Flanagan and Mercer, 1989; Galizia et al., 1999b), which we used as a reference for this study, the glomeruli nomenclature is based on afferent supply by one of the four antennal input tracts (T1–T4). According to these atlases, glomeruli were grouped into four clusters. In addition, special characteristics of terminal arborizations of ORN axons within the T4 glomeruli were used to identify glomeruli belonging to the T4 cluster. Within one cluster, glomeruli were classified into "primary" and "secondary" glomeruli following the definition of Rospars and Hildebrand (1992). They defined "primary" glomeruli as invariant glomeruli that can be found in each preparation and can be identified solely on the basis of their size, form, and position in relation to anatomical landmarks. "Secondary" glomeruli were defined as identifiable by their relative position to primary glomeruli plus their own anatomical peculiarities.

In this study, for 20 primary glomeruli and many secondary glomeruli in the T1 and T4 cluster, the available atlases could be effectively used for individual identifica-

tion. However, for a substantial number of glomeruli manual identification based on visual alignment did not work.

Especially in the T3 cluster, interindividual variance of number, shape, and characteristics of the glomeruli is relatively high (Flanagan and Mercer, 1989; our observations), which made it impossible to identify all glomeruli supplied by this tract. As an alternative, using a reconstruction based on doubly labeled preparations (see above) enabled us to perform a glomerulus-specific classification of the sensory input and uniglomerular output connectivity via the m- and l-ACT. In addition to the dendritic innervation pattern of PNs within the AL, we reconstructed the location of PN somata and assigned them to either the m- or the l-ACT population. For 3D reconstruction of glomeruli we used the Amira 3.1 feature "wrap." To reconstruct the sensory input tracts and ACTs as well as the position of PN soma clusters, we used the Amira features "interpolate" and "automatic threshold labeling."

Online material

Index of glomeruli. To allow comparison with the AL reconstructed most recently, we compiled an index of all glomeruli from Galizia et al. (1999b) and assigned them to the subpopulations defined by their efferent (m-, l-ACT) and afferent (T1–T4) supply as found in this study. This index is provided as online material. It includes a list of all 20 primary glomeruli that were identified in every preparation plus their anatomical description. For each other glomerulus of the Galizia reconstruction, we tried to define its affiliation to the m- or l-ACT hemisphere and to the correct sensory tract or subtract based on our antennal nerve mass-fill preparations.

Incorporation of data in the standard atlas of the honeybee brain. We incorporated our reconstructions of the ACTs and their arborizations within the MB calyx and LH into the published standard atlas of the honeybee brain (Brandt et al., 2005). For this, the neuropil outlines of several specimens were segmented and geometrically transformed into the Honeybee Standard Brain. The computed transformation values were then used to register 3D reconstructions of uPN-ACTs and their target projections in the MB-calyx and LH derived from three different specimen separately into the Honeybee Standard Brain (for a detailed description of the registration process, see Brandt et al., 2005). In a similar fashion the intracellularly stained antennal lobe feedback neuron (ALF-1) was fitted into the Honeybee Standard Brain (Figs. 6C, 8C, and online material). The Honeybee Standard Brain including parts of our data is available online at http://www.neurobiologie.fu-berlin.de/beebrain/.

3D model of the antennal lobe. A color-coded rotating 3D model of the AL (as described in the Results) including the antennal sensory tracts together with the input–output tract affiliation of all glomeruli (plus one version without the antennal input tracts) is available as digital online material. In addition, a digital confocal image stack of a doubly labeled AL preparation (mass fill of antennal sensory axons combined with l-ACT PNs, and m- and l-ACT mass fill) and a doubly stained MB calyx are available as online material (including a metafile with legends and software instructions).

RESULTS

Hemispherical organization of m- and l-ACT glomeruli

We double-labeled the m- and l-ACT with different dextran tracers (n = 4). A typical example of a successful staining is shown in Figure 2D–H (the complete confocal data stack is available as online supplementary material). The corresponding 3D reconstructions of glomeruli are shown in Figure 2A–C. Groups of glomeruli supplied by either the m- or the l-ACT are clearly segregating the AL into two hemispheres, supporting previous observations by Abel et al. (2001). Eighty-four glomeruli in the ventral-rostral hemisphere of the AL are innervated by PNs of the l-ACT (green) and their axons project dorsally, forming a single bundle on their way through the inner nonglomerular AL neuropil (consecutive slices in Fig. 2D–H). The l-ACT exits the AL dorsally, bends rostral-lateral, then projects toward the ipsilateral LH (green l-ACT reconstructed in Fig. 2A–C). Seventy-seven glomeruli located in the dorsal-caudal hemisphere of the AL are innervated by PNs leaving the AL through the m-ACT (magenta; Fig. 2A–C). Axons of the m-ACT PNs project rostrally and form two separated bundles on their way through the inner nonglomerular AL neuropil (Fig. 2G, and in another specimen, Fig. 2I). In the rostral-dorsal AL, these two subtracts bend around the l-ACT (Fig. 2H) and fuse before they exit the AL as the m-ACT (magenta m-ACT in Fig. 2A–C) into the rostral direction.

We found two large glomeruli on the dorsal side of the AL that were never labeled by retrograde staining of the m- and l-ACTs (n = 9; 4 double- and 5 single-labeled preparations). These glomeruli were identified as glomerulus D01 and D02 of the T4 cluster (after Galizia et al., 1999b). Presumably, the two glomeruli are not innervated by olfactory uPNs at all. In a single glomerulus, identified as B02 of the T2 cluster, we found arborizations of PNs from both the m- and l-ACT (n = 2).

All other glomeruli (except D01, D02, and B02) can be clearly separated by allocation to either the m- or the l-ACT, resulting in a hemispherical separation of the AL.

Soma clusters of m- and l-ACT projection neurons

Retrograde tracing labeled the somata of the PNs and allowed a 3D reconstruction and classification into ACT-specific clusters (Fig. 2). We found the somata of l-ACT PNs in a broad cluster along the AL rim around the l-ACT hemisphere (Fig. 2A–C, dark green; green dashed line in Fig. 2D–F). The number of somata of l-ACT PNs was estimated in a single preparation as ~290 somata plus 10–20 not clearly identifiable somata. The distribution of somata of the m-ACT PNs is mostly restricted to the m-ACT hemisphere (Fig. 2A–C, dark red) and was estimated as ~400 somata plus 30–40 not clearly identifiable somata. They can be further grouped into three clusters, the m-ACT soma clusters mSC1–3. Cluster mSC1 includes all PN somata in the "lateral passage" (after Pareto, 1972). There they are widely dispersed within a large dorsal-lateral somata cluster containing many local interneurons (white dashed line in Fig. 2D–H). Most somata of the m-ACT PNs are located in the dorsal-medial rim of the AL, similar to findings reported by Abel et al. (2001). Here they are densely packed and dispersed, with hardly any somata from unlabeled local interneurons compared to

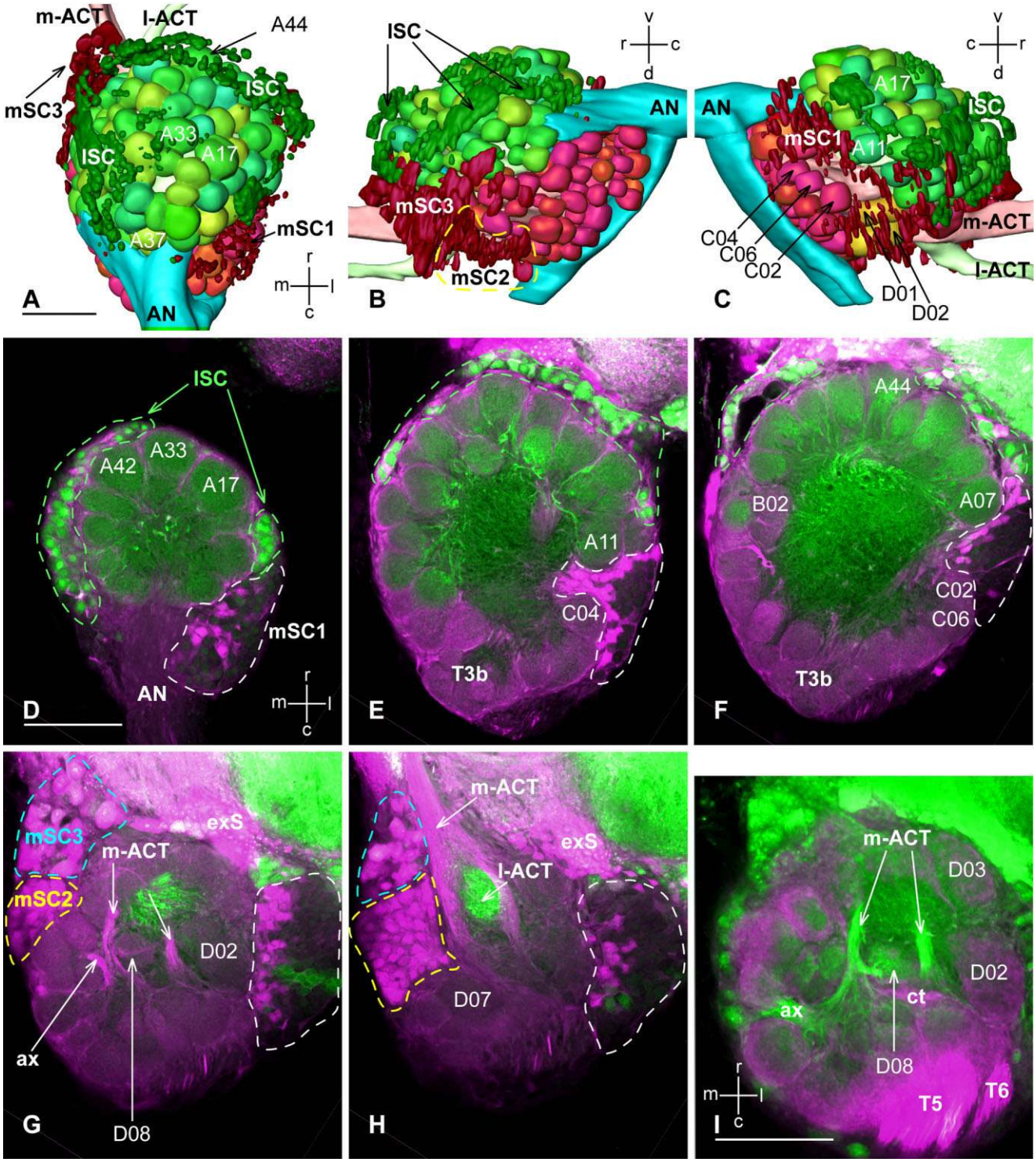

Fig. 2. Hemispheric organization of AL glomeruli by uPN innervation. Retrograde double labeling of the AL glomeruli via the m-ACT (magenta) and l-ACT (green). **A–C:** Reconstruction of the AL based on 135 optical sections at 2-μm intervals as in the examples shown in D–H. A: ventral, B: medial, C: lateral view. The glomeruli can be allocated into two hemispheres according to their efferent connectivity to either the m- or the l-ACT. Exceptions are the glomeruli B02 (F), that showed innervation via both ACTs, D01 and D02 (light brown in C) that were never stained (see text for further details). The reconstruction includes the positions of PN somata and their affiliation with either the m- (dark magenta) or l-ACT population (dark green). Somata of l-ACT neurons are found around the entire l-ACT hemisphere (lSC). Somata of m-ACT neurons aggregate in three different clusters (mSC1, 2 and 3). **D–H:** Orthoslices of the AL reconstructed in A–C, steps of 40 μm, showing glomeruli allocated to each hemisphere and the course of the origin of the m- and l-ACT within the AL. Axons of the l-ACT PNs project in dorsal direction through the inner AL and bundle together to form the l-ACT. Axons of the m-ACT PNs form two subtracts within the nonglomerular AL neuropil running around the crossing l-ACT (H) to finally fuse to the form the m-ACT. The uPN soma clusters are highlighted by dashed lines in green (lSC), white, yellow, and blue (mSC1, 2 and 3). Axons of mSC2 neurons enter the glomerular neuropil only via one bundle (ax in G,I). Note that protocerebral tracer injection also labeled some external neurons with their somata close to the AL neuropil (exS in G,H). In contrast to the described uPN soma clusters, these neurons had no axonal connection to the AL neuropil. A 3D confocal image stack is provided as online material. **I:** Efferent innervation pattern of a newly discovered glomerulus D08 in a double staining of the AL via the ORNs (magenta) and the m-ACT (green). Orthoslice through the dorsal AL (comparable to the depth in G). D08 lies rostral to the central tract (ct) and is intensely innervated by a side branch of the medial m-ACT subtract. AN, antennal nerve; m- and l-ACT, medial and lateral antenno-cerebral tract; T3b, position of the T3b glomeruli cluster; A17–D08, names of anatomically identifiable glomeruli; T5 and T6, dorsal tracts. Directions are indicated in the coordinate planes: rostral, r; caudal, c; ventral, v; dorsal, d. medial, m; lateral, l. Scale bars = 100 μm.

somata in the lateral passage. They can be further subdivided into two clusters. The somata of the mSC2 cluster form a densely packed, vertical layer, one to two cells thick, at the medial-dorsal side of the AL (yellow dashed line in Fig. 2B,G,H). They are characterized by a relatively uniform size and shape and by the projections of their neurites, which form one or two prominent bundles before they project through the glomerular layer in lateral direction to enter the nonglomerular AL neuropil (ax in Fig. 2G,I). The mSC3 cluster, separated from mSC2 by glial cells, includes all m-ACT PN somata situated in the medial-rostral end of the deutocerebrum. The neurons of mSC3 are densely packed, show more variation in size compared to the other clusters, and include relatively large somata (blue dashed line in Fig. 2G,H). The numbers of somata estimated from a single preparation were ~160 in mSC1, ~180 in mSC2, and ~60 in mSC3.

Afferent and efferent connection of glomeruli

To identify the sensory-tract affiliation of glomeruli belonging to the m- and l-ACT population, anterograde ORN mass-fills were combined with m-ACT backfills in two preparations and with l-ACT backfills in three other preparations. In all five preparations we found a very similar pattern of afferent and efferent connectivity of glomeruli. One doubly labeled AL (ORN axons and l-ACT) was completely reconstructed and a total of 163 glomeruli were counted (Fig. 3).

Comparison with earlier AL reconstructions by Galizia et al. (1999b) revealed several new anatomical details (see descriptions of details below) exemplified by three different specimens shown in Figure 4. The reconstruction of the AL, including the sensory innervation of all glomeruli, is shown in Figure 5A–E. The color code represents an affiliation to one of the four main antennal sensory tracts. Three consecutive slices through the AL in Figure 5G–I are examples of double-staining of ORN axons and one major ACT (here the l-ACT, same specimen as in Fig. 3), and is available as supporting online material.

T1 glomeruli. All glomeruli of the T1 cluster belong to the l-ACT hemisphere.

T2 glomeruli. The glomeruli of the T2 cluster split up into the two ACT hemispheres, visualized by the color code in Figure 5F. The two ventralmost glomeruli in our reconstruction are innervated by l-ACT PNs (white glomeruli, presumably equivalent to B04 and B05 in Galizia et al., 1999a). As mentioned above, glomerulus B02 is innervated by PNs of both ACTs (compare Fig. 2F with Fig. 5I for m- and l-ACT, respectively). All four other T2-glomeruli belong to the m-ACT hemisphere (yellow glomeruli in Fig. 5F).

T3 glomeruli. The glomeruli of the T3 cluster can be further subdivided into three clusters according to differences in their tract affiliation and sensory-innervation patterns. In the reconstruction the three clusters are indicated in three different colors. The T3a cluster (magenta in Fig. 5A–E) includes all glomeruli connected with one side branch of the AN, which branches off medially right after entering the AL and proceeds medial-rostrally around the outside of the glomerular layer (Fig. 5E, equivalent to tract "B3" in Pareto, 1972). The ventral glomeruli of the T3a cluster belong to the l-ACT hemisphere (10 in our reconstruction, bright pink in Fig. 5F), whereas the dorsal T3a-glomeruli belong to the m-ACT hemisphere (14 in our reconstruction, magenta in Fig. 5F). The T3b cluster (light brown in Fig. 5A–E) describes a population of glomeruli with unique anatomical features defined by four criteria: first, the location of the T3b glomeruli is somewhat separated from the general glomerular layer—they aggregate in a cluster caudal-dorsal to the T1 tract and medial to the dorsal tract that runs around the AL (Figs. 3D–G, 5B,E). Second, the average size of the glomeruli in the T3b cluster appears smaller than in any other region of the AL. Based on these two features, Arnold et al. (1985) termed this cluster "lobule." Third, the ORN axons innervating the T3b glomeruli split further caudal in the AN than in all other sensory tracts (compare, for example, with the origin of the T3a fibers; arrows in Fig. 4A–C). The fourth distinct feature shared by all T3b glomeruli is the difference in the innervation pattern of ORN-axon terminals. The ORN-axon terminals not only innervate the peripheral region of the T3b glomeruli, as is the case for most other glomeruli, but are also distributed in small densities across the entire core region of the glomeruli (glomeruli indicated by the dashed line in Fig. 4A–C). All glomeruli of the T3b population (12 in our reconstruction) belong to the m-ACT hemisphere. The remaining glomeruli in the lateral and dorsal region of the AL were grouped together in one subcluster, T3c (orange in Fig. 5A-E). All glomeruli of the T3c population (42 in our reconstruction) belong to the m-ACT hemisphere.

T4 glomeruli. A novel glomerulus-like structure was located in the T4 region of the AL, shown in Figure 4D–F. This glomerulus-like structure lies at the dorsal end of the AL, adjacent and rostral to the "central tract" (after Galizia et al., 1999b) (ct in Fig. 4D,F), and is clearly innervated by ORN axons belonging to T4. The arborization pattern of the ORN terminals is similar to the homogenous innervation pattern in T4 glomeruli D01–D06. Because of these two shared features we assigned this glomerulus-like structure to the T4 cluster and named it D08. Its reconstruction is shown in Figure 5B,C. The spheroidal shape of D08 also can be seen in retrograde labeling of its output connection (Fig. 2I). Dendrites of PNs from the m-ACT show dense arborizations within D08 and connect it via a prominent fiber bundle with the medial subbranch of the m-ACT. Surprisingly, glomerulus D07 did not show a homogenous ORN innervation or any connection to the T4 fiber network necessary to justify its assignment to the T4 cluster. In all of our preparations, glomerulus D07 showed an innervation pattern typical for all other T3c glomeruli that surround it: an innervated rim and a noninnervated core. Based on these two findings and its location within the T3c cluster, we reassigned D07 to the T3c cluster and renamed it C73. Arborizations of m-ACT neurons were found in 5 out of the 7 T4-glomeruli (D03–D06, and D08). As mentioned above, the glomeruli D01 and D02 may not be connected to the m- or l-ACT at all. The total numbers of glomeruli assigned to each cluster of the reconstructed AL are summarized in Table 1, row A. Table 1 also includes the distribution of the glomeruli within each cluster into the m- and l-ACT hemispheres (rows B–E).

Index of all glomeruli

The detailed register of all glomeruli is provided as a table in the online materials (Suppl. Table 1). Anatomical descriptions of identifiable glomeruli listed in the table are compared with those from Arnold et al. (1985), Flanagan and Mercer (1989), and Galizia et al. (1999b). Figure 2

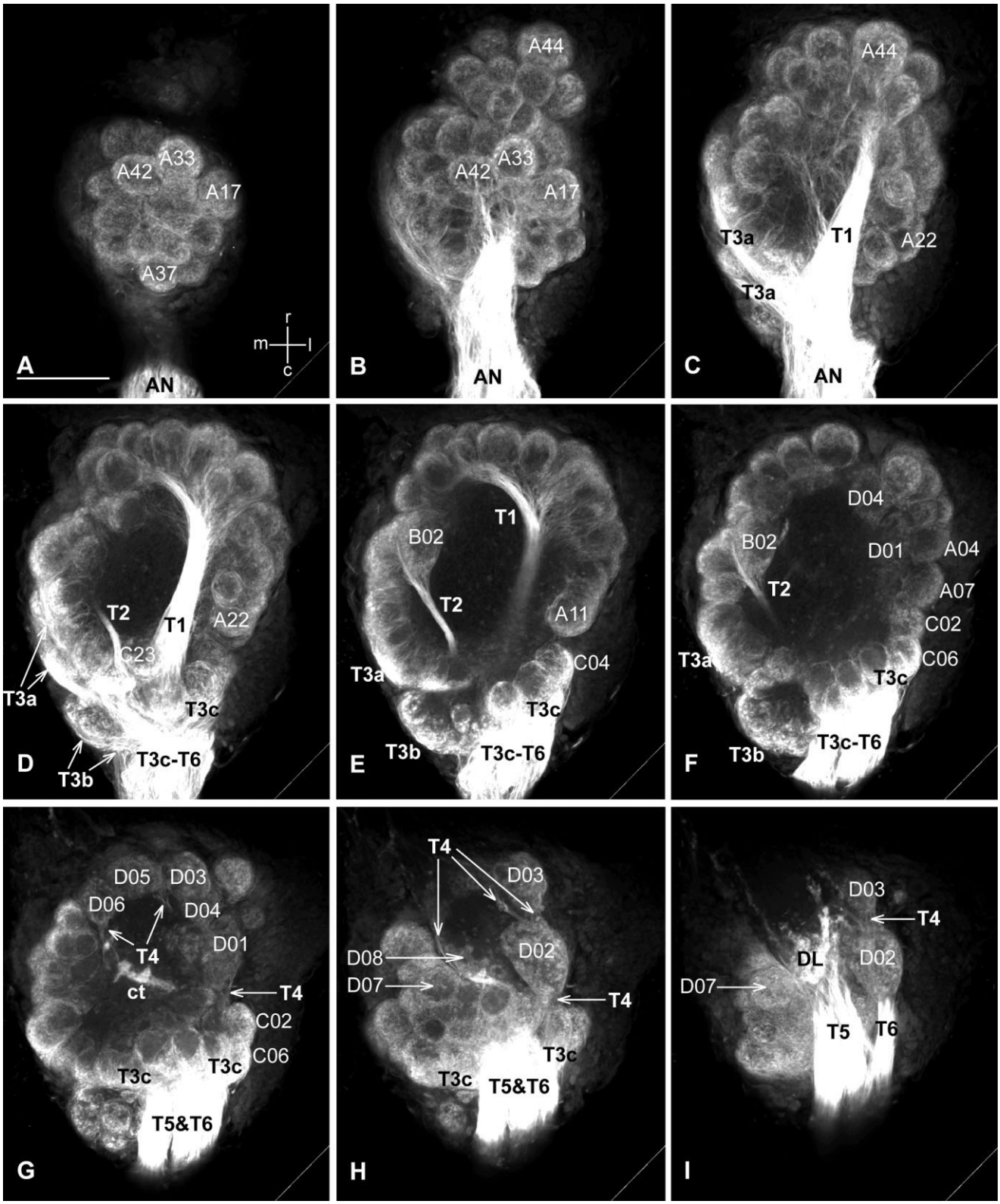

Fig. 3. Overview of the afferent innervation of the AL by the different sensory tracts including the positions of anatomically identifiable glomeruli. Projection views of 15 optical sections (30 μm optical thickness) from an anterogradely labeled AL. The different sensory tracts (T1–T4) innervate distinct glomeruli cluster. The dorsal tract T5 innervates the dorsal lobe (DL) and the targets of T6 are in the subesophageal ganglion and the dorsal protocerebrum (not shown). Note: T3 divides into three sub branches, T3a–c. Anatomically identifiable glomeruli are indicated (termed after Galizia et al., 1999b). AN, antennal nerve; ct, central tract. Scale bar = 100 μm.

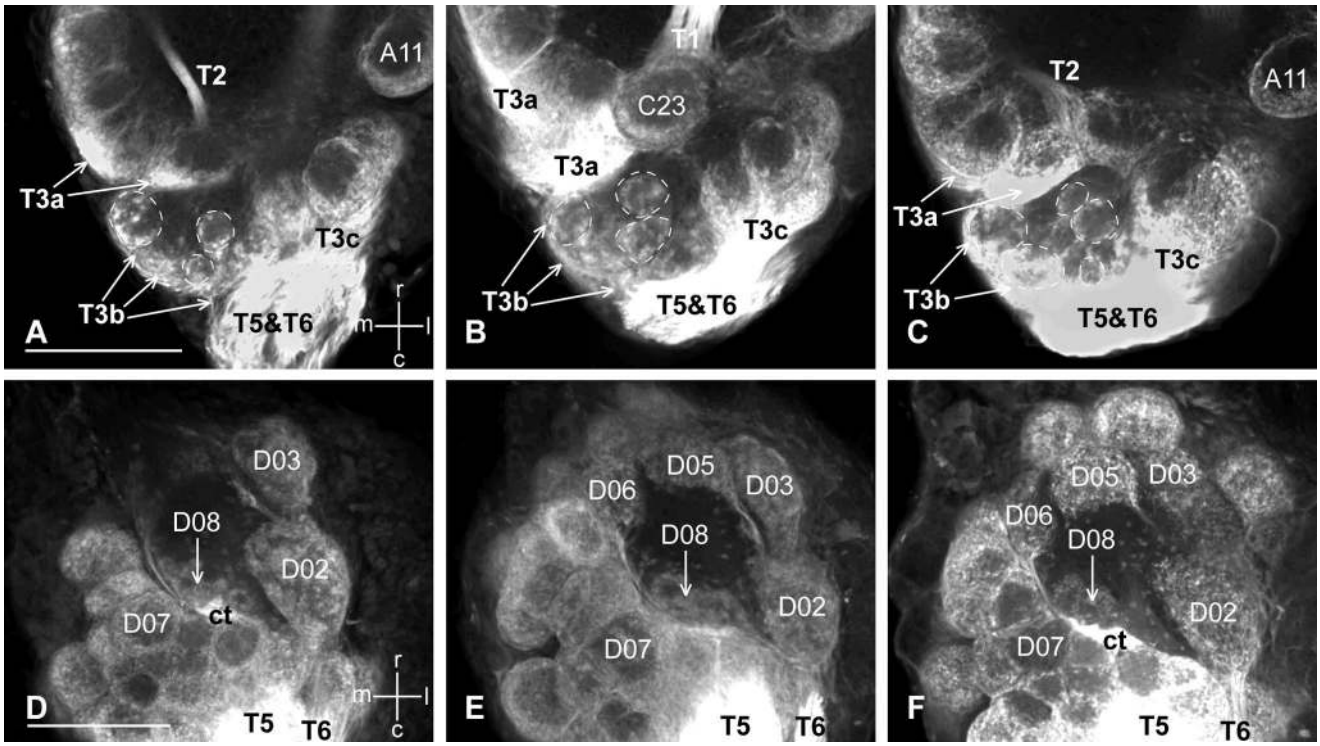

Fig. 4. Newly discovered features of the AL: the T3b glomeruli and the D08 glomerulus. Orthoslices of ALs from three specimen anterogradely labeled via the AN. **A–C:** Orthoslices of the caudal AL at depths between 100 and 120 μm showing the special features of T3b glomeruli. Glomeruli are grouped in a separate cluster adjacent to the dorsal tracts T5 and T6 and supplied by their own subtract (T3b). Glomeruli are smaller than the glomeruli in any other region of the AL. ORN arborizations in these glomeruli differ from the general scheme (exemplified by A11 in A and C). **D–F:** Orthoslices of the dorsal AL, at depths between 100 and 120 μm, showing position and arborization pattern of glomerulus D08. D08 has a reniform shape, 40–60 μm, and lies rostral to the central tract (ct). As the other T4 glomeruli D01–D06, it is supplied by the T4 tract system and shows a broad distribution of ORN terminals. Scale bars = 100 μm.

TABLE 1. Summary of the Afferent and Efferent Connection of Glomeruli

		T1	T2	T3a	T3b	T3c	Σ T3	T4	Σ
A	Σ T-cluster	72	7	24	12	42	77	7	163
B	l-ACT	72	2	10	0	0	10	0	84
C	m-ACT	0	4	14	12	42	68	5	77
D	both ACT	0	1	0	0	0	0	0	1
E	neither/nor	0	0	0	0	0	0	2	2

A Sum of all glomeruli belonging to a glomeruli cluster supplied by the sensory tracts and sub-tracts T1 – T4. **B,C** Affiliation of glomeruli in row A among the m- and l-ACT hemisphere. **D,E** Glomeruli belonging to both or none of the ACT hemispheres. A detailed table with a description of all individual glomeruli and a comparison with the data from Galizia et al. (1999b) and Flanagan and Mercer (1989) is provided as online material.

shows some of the 20 "primary" glomeruli we were able to identify (for further details, see Suppl. Table 1). In addition to splitting the T3 glomeruli into three subclusters and the (re-)assignment of glomeruli D07 and D08, we found the following differences compared to the cluster assignment by Galizia et al. (1999b), leading us to rename some glomeruli (for further details, see Suppl. Table 1).

Glomerulus B01: We never saw a T2-2 subtract, as described by Galizia et al. (1999b), and we therefore assigned glomerulus B01(1) to the T3a cluster (renamed C72) and B01(2) to the T1 cluster (renamed A73), based on their position in the glomerular arrangement.

Glomeruli C53 and C60: We further reassigned T3 glomeruli C53 and C60 to the T2 cluster (renamed B07 and B08), because they fit the location and characteristics of the two most dorsal T2 glomeruli we found in our preparations.

Segregation of olfactory input in the mushroom-body calyces

The course of the ACTs from the AL to their target neuropils in the protocerebral lobe is shown in the projection view in Figure 6A and the corresponding reconstruction in Figure 6C. The reconstruction is derived from different preparations scanned at several magnifications and registered individually into the frame of the Honeybee Standard Brain. The scheme in Figure 6B summarizes the connectivity pattern of the m- and l-ACTs (right side) and the ml-ACT network (left side).

The MB calyces receive their olfactory input from PNs of both the m-ACT (magenta in Fig. 6B,C) and the l-ACT (green in Fig. 6B,C). Both ACTs run in parallel ventrally around the distal end of the peduncle from where uPNs send collaterals into the calyces to form the inner ring

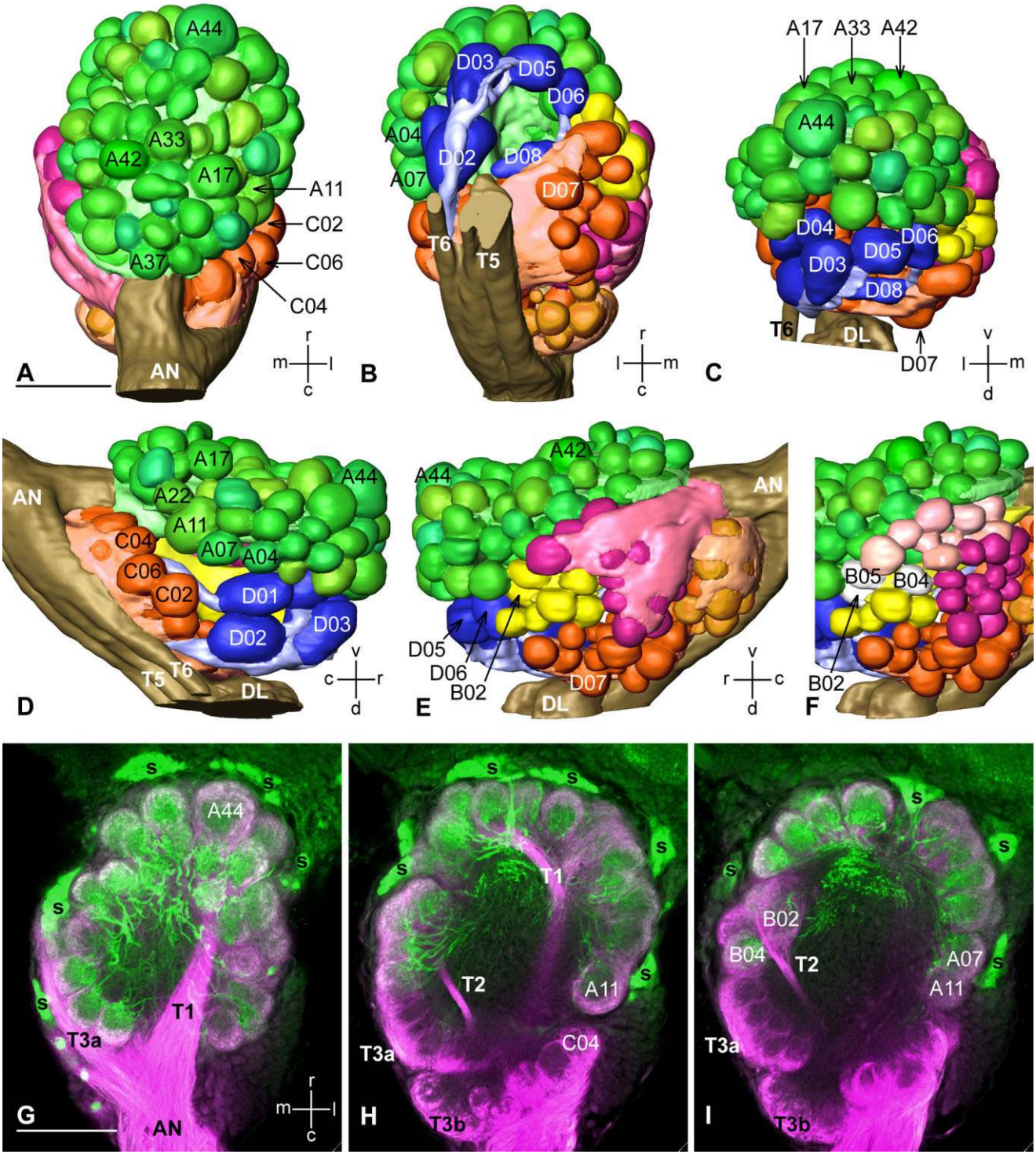

Fig. 5. Atlas of the AL glomeruli, including their affiliation with the sensory tracts and with m- and l-ACT. Double stainings of the AL via mass-fill of ORN axons and retrograde mass-fill of l-ACT PNs. **A–E:** Reconstruction of the AL, based on 142 optical sections. A: ventral, B: dorsal, C: rostral, D: lateral, and E: medial views. The color code represents the assignment of the glomeruli into six different clusters based on their afferent supply by sensory tracts 1–4 (also color coded) and/or special features in the ORN arborization pattern (for further details, see text). The T1-cluster (green) contains 72 glomeruli, the T2-cluster (yellow) includes 7 glomeruli, and the T4-cluster (blue) comprises 7 dorsal glomeruli connected to the T4 tract (bright blue). The T3 glomeruli are grouped into three subpopulations according to their afferent supply via the subbranches T3a (magenta, 24 glomeruli), T3b (light brown, 12 glomeruli), and T3c (orange, 42 glomeruli) (for further details, see text). T5 and T6 originate in the antennal nerve (AN) and project dorsally around the caudal surface of the AL toward the dorsal lobe (DL; all reconstructed in brown). The identification numbers of glomeruli (nomenclature after Galizia et al., 1999b) are included. A rotating version of the AL reconstruction is available as online material. **F:** Cut-out from E showing the separation of T2 and T3a glomeruli into the two ACT hemispheres. From 24 T3a-glomeruli, only the most ventral 10 belong to the l-ACT hemisphere (pink), all others belong to the m-ACT population (magenta and orange). From seven T2-glomeruli, two belong to the l-ACT hemisphere (white, B05 and B04) and four to the m-ACT population. A single glomerulus (B02) could not be clearly assigned to one hemisphere. **G–I:** Orthoslices of the AL that was used for the reconstructions in A–E at depths of 40, 80, and 150 μm showing the innervation profile of the sensory tracts (magenta) and the l-ACT (green). All T1 glomeruli are exclusively innervated by l-ACT PNs. The glomeruli of the T2- and T3a-cluster can be divided into the two ACT hemispheres. The T3b, T3c, and T4 glomeruli show no arborizations of l-ACT PNs and, hence, are assigned to the m-ACT hemisphere (except for glomerulus D01 and D02; see text for reasons). The somata of the l-ACT neurons (s) are also retrogradely labeled. A 3D confocal image stack is available as online material. Scale bars = 100 μm.

tract (IRT) (Mobbs, 1982). Consistent with the findings of Gronenberg (2001), only the inner half of the basal ring is innervated by collaterals of axons from PNs as shown in the cross section of the MB calyx in Figure 6D. After passing through the IRT that runs centrally along the collar, PN axons terminate in the lip region (Fig. 6C,E).

Double staining of the m- and l-ACT neurons (n = 3; Fig. 6F) revealed clear differences in the terminal arborization patterns of both ACTs. PNs of the m-ACT innervate the peripheral part of the olfactory basal-ring region, whereas PNs belonging to the l-ACT innervate the central part of the basal ring. On the basis of this difference in the PN termination, the basal ring can be further subdivided into three concentric layers according to its afferent supply: the outer basal ring receiving visual input (Gronenberg, 2001), the middle basal ring receiving olfactory input from the m-ACT PNs, and the central basal ring receiving olfactory input from l-ACT PNs. Slight overlap occurs among the border regions of the three sublayers.

The arborization patterns of the two PN populations differ in the lip of the MB calyces as well. l-ACT PNs innervate the central core of the lip region (Fig. 6CF) and leave an outer cortical layer noninnervated. PNs of the m-ACT innervate the whole lip region, but with very different density. The outer cortical area is very densely packed with synaptic buttons of m-ACT neurons, whereas the central core is very sparsely innervated. These observations lead us to the definition of two concentric subdivisions of the olfactory lip: the lip core innervated by PNs of both ACTs, but predominantly by l-ACT neurons, and the outer lip cortex exclusively innervated by PNs of the m-ACT (Fig. 6C).

Segregation of olfactory input in the LH

Similar to the olfactory input of the MB calyx, the LH shows an ACT-specific compartmentalization. Figure 6G shows a 3D reconstruction of the LH and its connections with the m-ACT (magenta), l-ACT (green), and the ml-ACT network (yellow). To view the various ACTs and their innervation pattern in 3D (Fig. 6C), see the Honeybee Standard Brain at http://www.neurobiologie.fu-berlin.de/beebrain/. Axons of m-ACT PNs remain bundled in a separated tract as they project parallel with the l-ACT. At the branching point of the l-ACT toward the LH the m-ACT bends ventrally toward the LH. The axons of the multiglomerular PNs that form the lateral network send off collaterals into the LH neuropil at multiple positions, with button-like structures found continuously along the connecting axons (defined below as "lateral bridge," lb in Fig. 6G,I–K).

Within the LH up to four compartments can be distinguished according to their innervation profile by different ACTs. They are shown in a series of consecutive sections in Figure 6H–K. m-ACT axons predominantly terminate in a restricted medial compartment of the LH neuropil (#1 in Fig. 6H–K). Moreover, the pear-shaped compartment #1 is exclusively innervated by uPNs of the m-ACT (Fig. 6G,H). The most rostral compartment #3 does not show any innervation by m-ACT neurons, but dense innervation by PNs of the l-ACT and PNs of the ml-ACTs 2 and 3. Between these two areas, another compartment (#2) can be distinguished by its innervation pattern. PN collaterals of the m-, l-, and ml-ACTs 2 and 3 form terminals, but less frequent than in the two adjacent compartments #1 and #3. A small area distal of compartment #3 shows a similar innervation pattern as #2 and is indicated as #2b in Figure 6J.

In the example shown in Figure 6G–K, all ACTs except ml-ACT 1 were stained. ml-ACT 1 leaves the m-ACT soon after it exits the AL and runs across the caudal protocerebrum to terminate in the medial part of the LH (Fig. 7). Comparison with ml-ACT 1 projections from other preparations (n = 4) led us to the assumption that a fourth LH compartment may exist next to compartment #1, which may be predominantly innervated by PNs of ml-ACT 1 (#4 in Fig. 6I–K).

Lateral network of multiglomerular projection neurons

Axons of PNs that leave the AL via several ml-ACTs exhibit a very characteristic arborization pattern on their way through the lateral protocerebrum, which was consistently found across individuals (n = 7) and will be described as the "lateral network" of the olfactory pathway. The three ml-ACTs contribute to this lateral network as follows (Figs. 6C, 7).

ml-ACT1. Three major ml-ACTs can be distinguished: The ml-ACT1 branches off the m-ACT first, right after it exits the deutocerebrum and crosses transversally through the caudal-lateral protocerebrum at a depth of 125–160 μm (from the surface) toward the medial LH (Fig. 7E,F). It has no side branches along its path and innervates solely the LH neuropil, predominantly its medial compartment #4.

ml-ACT2. The ml-ACT2 branches off the m-ACT about 100 μm behind ml-ACT1 and runs in parallel along the caudal-lateral surface of the MB peduncle at a depth of 200–230 μm (Fig. 7F,G). Along its transversal course, neurons of the ml-ACT2 send collaterals in rostral directions, in particular, around the vertical lobe, into the lateral protocerebral lobe, and even further toward the bases of both calyces. The remaining axons in the ml-ACT2 bend caudally again and terminate in the LH. The projection patterns of the ml-ACT 1 and 2 are schematized in Figure 7A.

ml-ACT3. The ml-ACT3 comprises a network of at least four distinct tracts (ml-ACT3a-d in Fig. 7G–I) running below the medial lobe and peduncle of the MB. Each subtract branches off the m-ACT at a different position and projects transversally toward the LPL at a depth between 270 and 350 μm. The neurons of the ml-ACT3 complex send collaterals rostrally around the dorsal peduncle toward the bases of the calyces (Fig. 7G–I) and in ventral directions toward the ventral protocerebrum and the ring neuropil surrounding the vertical lobe. Many axons of the ml-ACT3 network also terminate within the LH neuropil. The projection patterns of the four subtracts of the ml-ACT3 network are schematized in Figure 7B.

Ring neuropil. The innervation pattern of the PNs of the ml-ACT 2 and 3 allows discrimination of at least three different regions within the lateral protocerebral lobe with a dense accumulation of axons and axonal terminal branches. Most ventral in the brain, around the vertical lobe of the MB, axons and terminals of ml-ACT PNs form the "ring neuropil" (Abel et al., 2001) (rn in Fig. 7C,E). The ring neuropil has a thickness of ~25 μm, starts at a depth of 40–100 μm, and ends at a depth of ~180 μm.

Triangle. Axons that supply the ring neuropil all originate from an adjacent region that lies further dorsal and lateral in the protocerebrum, spanning a depth of 110–170

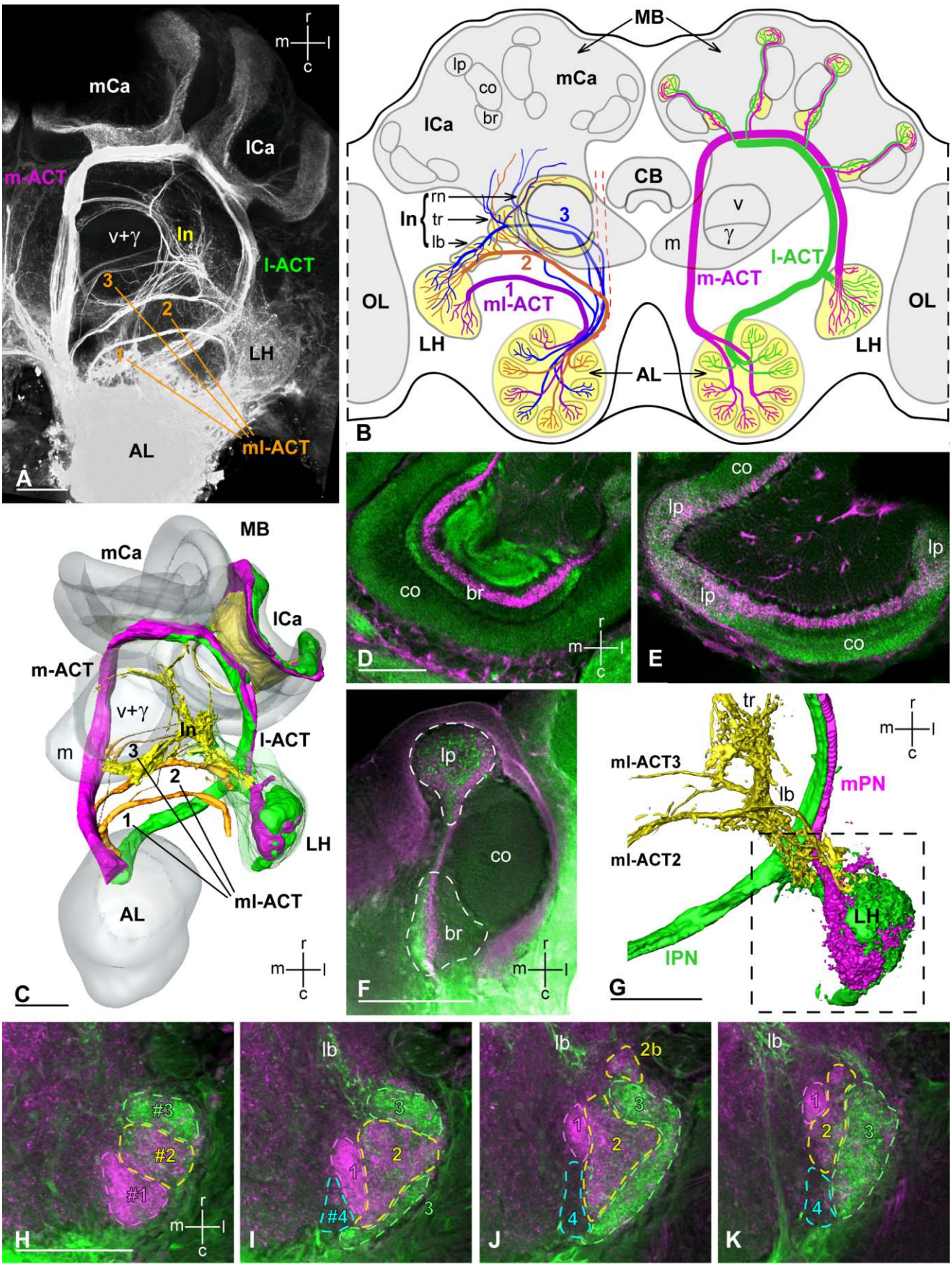
A
mCa
lCa
m-ACT
v+γ
In
l-ACT
3
2
1
LH
AL
mI-ACT
r
m
l
c
B
MB
lp
co
br
mCa
lCa
CB
rn
tr
lb
In
3
2
1
mI-ACT
v
γ
m
m-ACT
l-ACT
OL
LH
AL
C
MB
mCa
lCa
m-ACT
v+γ
In
l-ACT
m
3
2
1
LH
AL
mI-ACT
D
co
br
E
co
lp
lp
lp
co
F
lp
co
br
G
tr
mI-ACT3
lb
mPN
mI-ACT2
LH
lPN
H
#3
#2
#1
I
lb
3
2
1
#4
3
J
lb
2b
3
1
2
4
K
lb
1
2
3
4

Figure 6

μm. We termed this region the "triangle" (tr in Fig. 7E,F). The triangle describes a small region, only ~60 μm in diameter, in the center of the LPL. This region is densely innervated by collaterals of ml-ACT 2 and 3, which enter this neuropil from the dorsal side. Many axons pass through the triangle toward the ring neuropil or bypass the triangle laterally toward the LH.

Lateral bridge. On their way toward the LH, collaterals fan out to form a third neuropil, which we termed the "lateral bridge" (lb in Fig. 7F). The lateral bridge represents the tissue between the triangle and the LH and is a major route of MB extrinsic neurons of the vertical lobe (Rybak and Menzel, 1993; Strausfeld, 2002). It is located at a depth of 170–250 μm, spans a distance of ~110 μm from triangle to LH, and has a diameter of up to 60 μm.

All three neuropils contain many axonal terminals with bouton-like structures at a higher density than in any other region of the lateral protocerebral lobe except the LH. All three neuropils are shown in a projection view of the lateral protocerebral lobe (Fig. 7C) and in the schematic drawings of the lateral network they form in Figure 7A,B. Figure 6B gives an overview of the olfactory pathway that connects the AL with the protocerebrum showing the m- and l-ACT on the right side and the ml-ACTs on the left side. Here, the multiglomerular distribution of the ml-ACT afferents within the AL is adapted from the results of previous studies (Fonta et al., 1993; Abel et al., 2001).

It is important to mention that our mass-fills of the antenno-cerebral connections always labeled a group of 5–12 somata at the dorsal surface of the brain, ~10 μm in diameter (Fig. 7I). Their axons run separately through the protocerebrum at depths of 320–390 μm and originate from an unknown region of the deutocerebrum.

Single antennal lobe feedback neuron

Since our tracing technique labeled both anterograde and retrograde connections between the deuto- and protocerebrum, the preparation shown in Figures 6A and 7 also includes neurons originating in the protocerebrum with projections and arborizations in the AL. The group of dorsal somata mentioned above is an example of such retrogradely stained neurons. Another prominent neuron that appeared repeatedly in our preparations was a neuron that connected the MB and protocerebrum with the antennal lobe (Figs. 6A, 7D; antennal lobe feedback neuron, ALF-1). This neuron was also found in a single neuron fill from an intracellular recording (Fig. 8B). The neuron has a large soma (~20 μm in diameter) at the ventral surface of the brain, right next to the vertical lobe, which was also found in many of our mass stainings (s in Figs. 6A, 7D). Following the course of its neurite we could identify its projections within the AL (ax in Fig. 7D,E). The prominent process in the protocerebrum proceeds between vertical lobe and the medial calyx and runs counterclockwise around the vertical lobe toward the soma. Comparing several mass fills of the antenno-cerebral connections (n = 5), we conclude that each brain half contains a single ALF-1 neuron (Fig. 8A).

Comparison of the mass fills with the intracellular staining revealed further anatomical details of this neuron. Processes of the ALF-1 neuron innervate distinct parts of the LPL: the ring neuropil and the triangle (rn, tr in Fig. 8A,B). Other arborization regions were found in the rostral protocerebrum and the distal end of the peduncle of the MB (arrowheads in Fig. 7E). Another innervated region was a distinct band within the vertical lobe (arrowheads in Figs. 7E, 8A). This band seems equivalent to the caudal band of the vertical lobe described in Strausfeld (2002), the output region of class 1 Kenyon cells from the calyx lip. After circling around the vertical lobe to the soma, the neurite bends toward the deutocerebrum and enters the AL outside any ACT, although close to the m-ACT. Dense arborizations of the ALF-1 neuron span across the entire AL, with most prominent branches in the inner, nonglomerular neuropil and fine branches with blebs that appear to reach into the basal part of glomeruli (Fig. 8B). An intracellular recording and staining of a neuron reported by Iwama and Shibuya (1999) shows many similarities to the ALF-1 neuron described here,

Fig. 6. Projections of m- and l-ACT in the mushroom-body calyx and lateral horn. **A:** Projection view of an anterograde mass-fill of all ACTs. Projection of the two major m- and l-ACT from the AL to the medial and lateral calyces (mCa, lCa) of the MB and the LH. The three ml-ACTs 1–3 branch off the m-ACT sequentially and innervate the LPL to form the lateral network (ln) that spans from the vertical lobe (v+g) to the LH. **B:** Schematic overview of the central olfactory pathway in the honeybee. The left side shows the projection of the multiglomerular ml-ACT1, 2 and 3 (purple, brown-orange, blue), which receive their input from many glomeruli across the AL. Each ml-ACT branches of the m-ACT at a different position (indicated by the dark-red dashed line). The protocerebral target areas of the ml-ACTs (yellow) are the LH and the LPL. In the LPL three innervation foci, the ring neuropil (rn), triangle (tr), and lateral bridge (lb), can be distinguished. Together with the ml-ACTs they contribute to a discrete lateral network (ln). The right side shows the projection of the m- and l-ACT. Both tracts comprise uniglomerular PNs receiving input from glomeruli in two separated hemispheres of the AL (Fig. 2). The protocerebral target neuropils (yellow) are the basal ring (br) and lip (lp) of the MB calyces and the LH. Projection patterns of m- and l-ACT neurons differ significantly with regional overlapping (for details, see text). OL, optic lobes; CB, central body; m, medial; v, ventral; γ, gamma-lobe. **C:** 3D reconstruction of the preparation in A showing the m-ACT in magenta, the l-ACT in green, and the ml-ACTs in yellow/orange in combination with MB and LH projections of the uPN-ACTs. Reconstructions are derived from three different preparations and geometrically transformed into the Honeybee Standard Brain (Brandt et al., 2005; http://www.neurobiologie.fu-berlin.de/beebrain/). The lateral network is formed by collaterals of the ml-ACT 2 and 3 yellow. For a detailed description of the lateral network, see text. **D,E:** Anterograde mass-fill of both major ACTs label innervation of the MB (magenta) combined with anti-synapsin immunofluorescence (green). Vertical orthoslices through the lateral calyx at its dorsal end, cutting the basal ring region (br) in D and the lip region in E (lp). co, collar. **F:** Double labeling of the m-ACT (magenta) and the l-ACT (green) showing differences in their innervation pattern in the MB basal ring and lip (see text for further details). A 3D confocal data stack is provided as online material. **G:** Double labeling of the m-ACT (mPN in magenta) and the l-ACT (lPN in green) showing differences in their innervation foci in the LH. Due to methodical restrictions ml-ACT 2 and 3 were also labeled and appear in yellow in the reconstruction. tr, triangle; lb lateral bridge. **H–K:** Consecutive orthoslices through different depths of the LH shown in G (marked by the dashed square). PNs of the m-ACT (magenta) exclusively innervate compartment #1, but not compartment #3, which is defined by innervations of the l- (green), ml-ACT 2 and 3. Compartment #2 receives olfactory input from both the m- and l-ACT. Medial to #1 we suggest a forth compartment that receives its input from the ml-ACT1 (not labeled here). Scale bars = 100 μm.

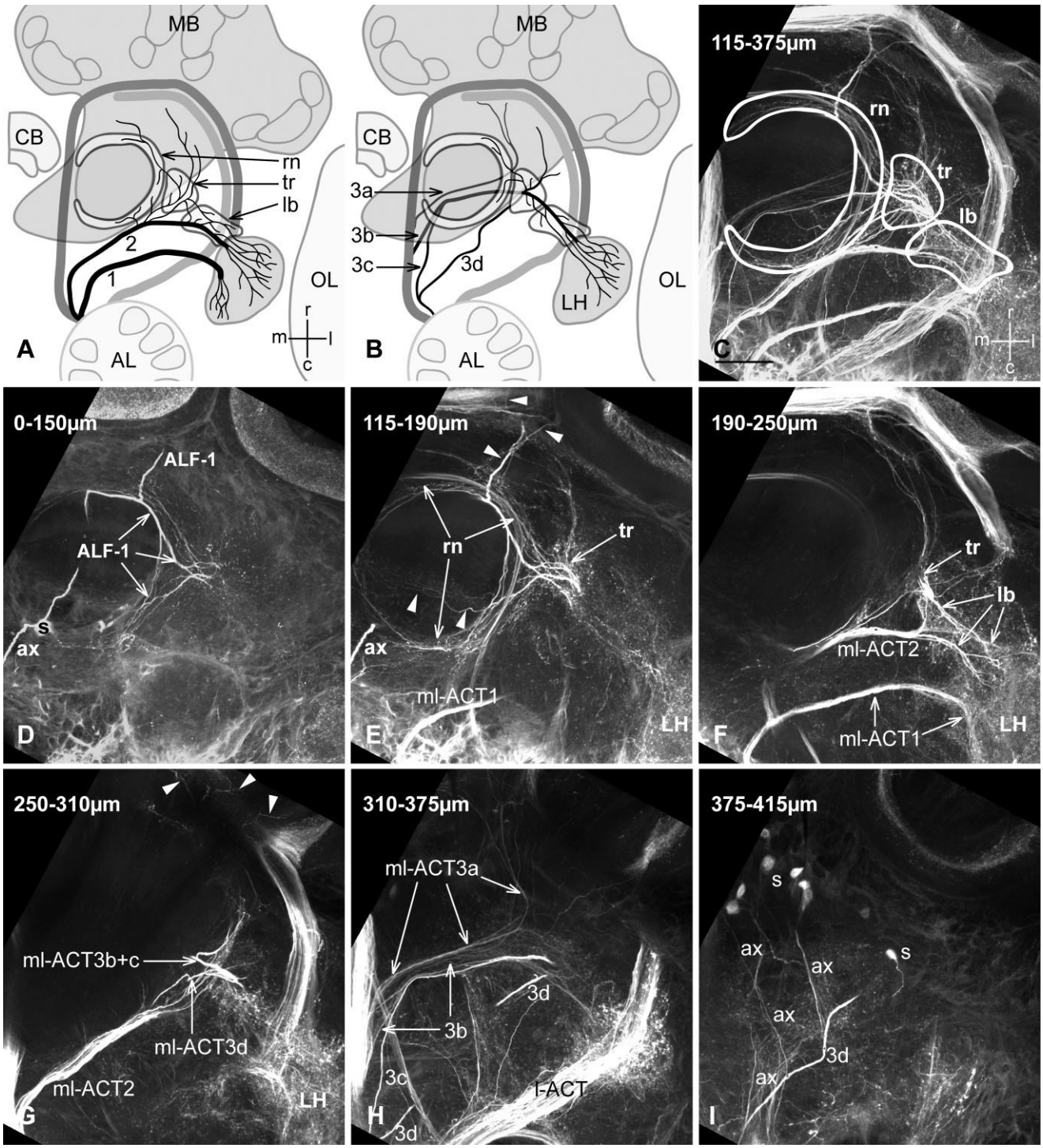

Fig. 7. Anatomy of the ml-ACTs and the lateral network within the protocerebrum. **A,B:** Schematic drawing of the innervation patterns of the ml-ACT1 and 2 (A) and of the ml-ACT3 tract system (B), as exemplified in Figure 6C–I. Their innervation targets include the LH, the ring neuropil (rn), the triangle (tr), and the lateral bridge (lb). The latter three are distinct innervation foci within this lateral network of ml-ACTs. For orientation, MB, AL, LH, the optic lobes (OB), and the central body (CB) are shown. **C:** Projection view of an anterograde mass-fill of all ACTs, showing a cutout of the LPL. Three areas of intense innervation by the ml-ACT 2 and 3 can be distinguished: the ring neuropil, the triangle, and the lateral bridge. **D–I:** Consecutive projection views of the LPL in C showing the lateral network in different depths. The ml-ACT1 branches off the m-ACT first and projects to the LH without collaterals (E,F). Second, the ml-ACT2 leaves the m-ACT and projects toward the LPL and the LH (F,G). The ml-ACT3 comprises at least four small axon bundles that branch off the m-ACT (ml-ACT3 a and b) or originate in the AL directly (ml-ACT3 c and d) (G–I). These axons either project to the LPL and contribute to the lateral network or innervate the LH. Note that the AL mass-backfill also retrogradely labeled protocerebral cells, the "antennal lobe feedback neuron 1" (ALF-1 plus its axon (ax) in D; arrowheads in E) and several somata at the dorsal end of the brain (s and ax in I). The numbers in the right upper corner of C–I indicate the depth of each section. Scale bar = 100 µm in C (applies to D–I).

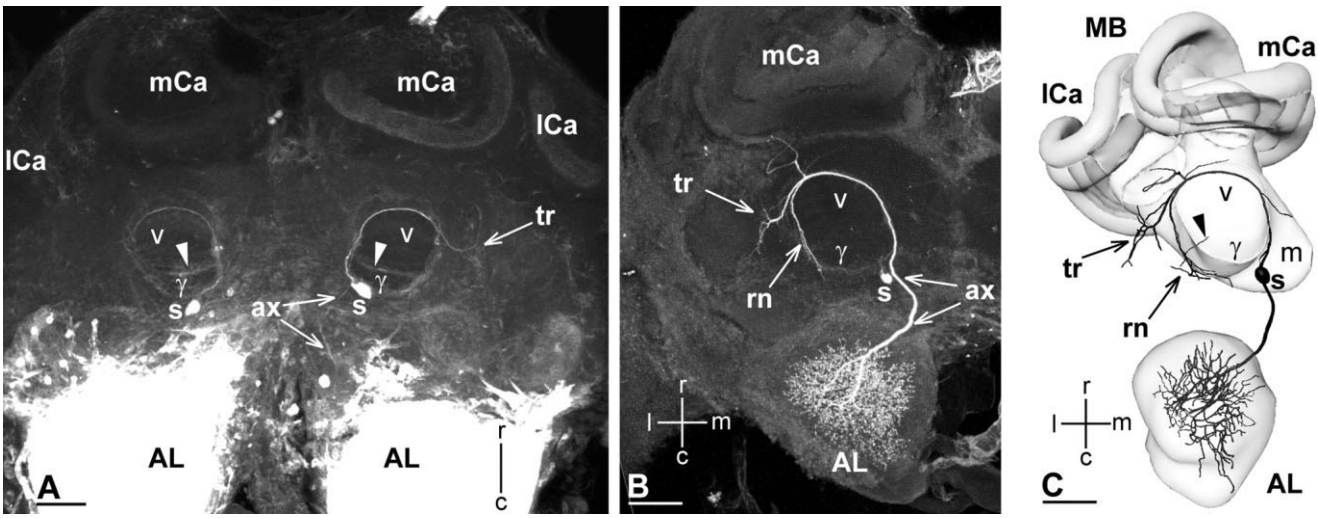

Fig. 8. The morphology of ALF-1, a unique centrifugal neuron. **A:** Projection view of a mass-fill of all AL connections with the protocerebrum showing the ventralmost section of the brain. In each half of the brain only one soma (s) can be found around the vertical lobe, proving that the ALF-1 neuron is unique in each hemisphere. Additionally, the axonal projection (ax) toward the AL and around the vertical lobe toward the LPL can be tracked. The position of the triangle (tr) is marked by an arrow. Arrowheads mark the innervated band within the vertical lobe (v) at the border of the gamma lobe (γ). **B:** Projection view of a single ALF-1 neuron labeled with Lucifer yellow. This cell matches the projection pattern and the position of the soma from the cells in A and Figure 7D,E. Its terminals within the AL have bleb-like structures, in contrast to the fine and smooth endings in the protocerebrum, which identifies the AL as the output region. The boutons are distributed across the whole AL, innervating almost all glomeruli, but having also extensive branchings in the inner nonglomerular neuropil. In the protocerebrum the ALF-1 neuron innervates the ring neuropil (rn) the triangle (tr) and the vertical lobe and peduncle of the MB. **C:** Reconstruction of the ALF-1 neuron shown in B after incorporation into the Honeybee Standard Brain (Brandt et al., 2005). The arrowhead marks the side branch innervating a certain band in the vertical lobe, as it is visible in single orthoslices but not in the projection view in B; also compare with the band marked by arrowheads in A and Figure 7E. A rotating 3D image of this neuron is available as online material. Scale bars = 100 μm.

although the soma of was not stained. A 3D reconstruction of the ALF-1 neuron aligned in the Honeybee Standard Brain is presented in Figure 8. A rotating movie of this neuron is provided as online material.

DISCUSSION

The aim of this study was to define the input–output relationship of the medial and lateral ACT in the honeybee brain and to analyze the projection pattern of all ACTs in higher centers of the protocerebrum. The most important results of this study are that the uPN output pathways (m- and l-ACT) receive input from two clearly defined sets of olfactory glomeruli clustered in two AL hemispheres, and that the projections of m- and l-ACT uPNs remain largely segregated in the MB-calyx lip and basal ring, and in the LH, with only some regions of overlap. In addition, this study revealed novel features of the AL anatomy and of the projections of ml-ACT multiglomerular PNs in a "lateral network" within the lateral protocerebrum. Finally, we discovered a novel feedback neuron between the protocerebrum and the AL.

Input–output relationships of antennal lobe glomeruli

Comparison of our results with previously established AL reconstructions (Flanagan and Mercer, 1989; Galizia et al., 1999b) revealed novel information about the input–output relationship of AL glomeruli. The two uniglomerular ACTs connect all AL glomeruli (except for D01 and D02) with the ipsilateral MB calyces and LH. The input of both tracts is clearly segregated in two hemispherical clusters of glomeruli, which was indicated in the study of Bicker et al. (1993) and Abel et al. (2001). The glomeruli of the T3a-cluster and of the T2 cluster are divided in uPNs of both m- and l-ACTs, and the B02 glomerulus was found to be connected to both tracts.

In addition, within the m-ACT hemisphere the glomeruli in the T3b and the T4 cluster have anatomical peculiarities indicating that these glomeruli might process input from either other sensory modalities (e.g., taste, temperature, humidity) or odors in a different way.

Tracing of the projections of hygro- or thermosensitive sensilla or PNs responding to these modalities, as performed in the cockroach (Nishikawa et al., 1995; Nishino et al., 2003), or of receptor neurons of gustatory sensilla may help to reveal the function of these anatomically different glomeruli. Responses of uPNs to temperature and moisture were also reported for the honeybee, but the neurons were not assigned to the l- or m-ACT (Itoh et al., 1991). Abel et al. (2001) described a bilateral PN with dendritic arbors in the T4 region that did not respond to odors, but to antennal contact stimulation with beeswax, which provides further support for a possible role of the T4 glomeruli in contact-chemoreception.

In *Diptera* (Stocker et al., 1990; Anton et al., 2003) and *Lepidoptera* (Kent et al., 1999), differential innervation of glomeruli by antennal, maxillary, or labial palp afferents indicates some degree of organotopic organization of the AL. Anton et al. (2003) and Ignell et al. (2005) hypothesized that in the *Holometabola* two separate glomerular neuropils, the AL and the dorsal *Lobus glomerulatus*

found in *Hemimetabola* like *Blattaria* and *Orthoptera*, became fused (Ernst et al., 1977; Hansson and Anton, 2000; Ignell et al., 2000). Hymenoptera have only rudimentary maxillary palps, but the labial palps evolved to form the outer shaft of the proboscis. Labeling of the labial nerve in the honeybee would provide further evidence for an organotopic organization and possible fusion of the AL. Among the dorsal glomeruli in the honeybee AL, D01, D02, and D08 are the best candidates for nonolfactory or multimodal glomeruli.

Functional considerations of a dual olfactory pathway

The odor specificity of a glomerulus is primarily defined by the odorant receptors of ORNs innervating it. Five to 35 ORNs are colocalized in individual pore plate sensilla (Schneider and Steinbrecht, 1968), and the axons of individual ORNs from single pore plates terminate in different glomeruli (Kelber et al., 2006). Axons from single pore plate sensilla were found in all sensory tracts T1–T4, but T1 and T3 were the most frequent pathways. This tract-specific division of ORN axons may indicate that olfactory input is sorted into global categories within the AL. Interestingly, all T1 glomeruli belong to the l-ACT hemisphere, and the vast majority of T3 glomeruli belong to the m-ACT. Functional studies are needed to find out whether similar or different olfactory input is transferred via these two major tracts. For technical reasons, calcium imaging studies were so far only able to characterize mainly l-ACT glomeruli supplied by T1 (Joerges et al., 1997; Galizia and Menzel, 2000; Sachse and Galizia, 2002; Galizia and Kimmerle, 2004).

Müller et al. (2002) found differences in the temporal discharge patterns and tuning properties of individual m- or l-ACT uPNs. The authors hypothesized that the l-ACT could be a fast unspecific route and the m-ACT a more specific, but comparatively slower pathway resulting in parallel processing of different aspects of the odor stimulus. However, the data of Müller et al. (2002) may be biased by a selection of odors for stimulation of m- or l-ACT neurons, and the differences found in m- and l-ACT uPN responses may be caused by odor selection rather than processing of different aspects of an odor stimulus along the two tracts.

ORNs drive the PN responses in a corresponding glomerulus via direct activation, and indirect activation via local interneurons distributes information about the stimulus across the AL, which may result in a complex temporal pattern of uPNs. The resulting combinatorial code carried by the m- and l-ACT represents "parallel processing" by its nature, but are the uPN populations of the m- and l-ACTs qualitatively different in the way they convey information about the stimulus, as suggested by Müller et al. (2002)? The sets of uPNs innervating different groups of glomeruli have different receptive fields, primarily based on the odor specificities of ORNs that innervate these glomeruli. This, however, does not necessarily yield qualitative different ways the uPNs convey information. For true parallel processing of odor information, the m- and l-ACT uPNs should differ by either 1) different input connectivity within an glomerulus, or 2) different intrinsic properties, or 3) AL network properties separating different aspects of an odor stimulus. So far, none of the mentioned preconditions have been demonstrated or are supported by neuroanatomical data.

Since it is not known whether the m- and l-ACT hemisphere receive similar of different odor information and whether uPNs of the m- and l-ACT differ in their intrinsic physiological properties, we prefer the term "dual olfactory pathway" as a more general term compared to "parallel pathway." Future studies on the odor response profiles of m-ACT glomeruli are needed to address this question. Furthermore, tract-specific labeling of uPN somata may be used as a tool in future patch-clamp studies on isolated AL neurons to address this question (Grünewald, 2003). Some information is available on a potentially differential distribution of neurotransmitters in the different tracts. Only the m-ACT was shown to contain acetylcholinesterase staining, and the MB lip showed immunoreactivity to an acetylcholine receptor-like antigen, suggesting acetylcholine as the main transmitter of the m-ACT (Kreissl and Bicker, 1989). In addition, few GABAergic fibers were found along the m-ACT and ml-ACT, indicating that some of the AL PNs might be GABAergic, and a GABAergic bridge was shown between both ALs (Schäfer and Bicker, 1986). The transmitter or neuromodulator systems of the l-ACT and ml-ACT are largely unknown and need to be the focus of future studies.

Dual pathway of olfactory input to the mushroom bodies

Based on staining of two individual uPNs in different individuals and their computer-aided alignment, Müller et al. (2002) assumed that arborizations of m- and l-ACT neurons largely overlap in both the MB-calyx lip and basal ring. Our double stainings revealed a clear segregation in the calyx innervation patterns. However, a closer look at the original reconstructions in figure 1a,b of Müller et al. (2002) and figure 7 in Abel et al. (2001) indicate differences in the anatomy of the m- and l-ACT neurons similar to the pattern we found here.

Does the input to the MB calyx remain segregated at the level of MB intrinsic neurons? The three calyx subdivisions are differentially innervated by three populations of class 1 (spiny) Kenyon cells (c1KCs), which extend axons to the MB lobes. A concentric arrangement of calycal zones is transformed into a stratified arrangement of c1KC axons in the lobes (Mobbs, 1982; Strausfeld, 2002). Consequently, each calyx subdivision is represented by one specific layer in the medial and vertical lobe (Strausfeld, 2002). Strausfeld (2002) divided lip, collar, and basal ring into further subdivisions and proposed corresponding substrata in the vertical lobe. In contrast, the narrow dendrites of class 2 (clawed) Kenyon cells (c2KC) with somata outside the calycal walls (see also Rybak and Menzel, 1993) are distributed across the entire calyx, and their axons commonly project to the gamma lobe. In the honeybee, the gamma lobe is fused with the vertical lobe and represents its most ventral layer (Strausfeld, 2002). Strausfeld (2002) found c1KCs with dendrites extending across the entire lip regions, whereas others were restricted to the inner or peripheral portion of the calyx lip. The m-ACT innervated rim of the lip corresponds well with the outer lip zone described by Strausfeld (2002) and the "outer layer" found by Gronenberg (2001).

The basal ring is also subdivided into two zones based on the distribution of several c1KC types: the outer and the inner zone, each represented by distinct strata in the basal ring division of the lobes (Strausfeld, 2002). Gronen-

berg (2001) described a similar zonation of the basal ring based on its afferent supply: an outer visual zone and an inner olfactory zone receiving input from AL uPNs. We found that the olfactory part of the basal ring can be further subdivided into the m-ACT and l-ACT input areas, which correspond well to the two layers of the inner zone in Strausfeld (2002).

Combining the previous findings with the results of our present study we conclude that in both the lip and the basal ring distinct subpopulations of c1KCs are likely to further transfer olfactory input via two c1KC channels to distinct strata within the vertical and medial lobe of the MBs. In addition, class 2 (clawed) KCs may represent a third pathway integrating both m- and l-ACT input and sending it to the gamma lobe. Segregation of olfactory input throughout the MBs could have important implications for olfactory associative tasks, as the MBs are important for learning, memory, and behavioral plasticity (reviewed by Menzel, 2001; Heisenberg, 2003; Fahrbach, 2006). Similarly, Tanaka et al. (2004) suggested a zonal organization of the MB calyx in *Drosophila*.

Multiple pathways of olfactory input to the lateral horn

Our results suggest at least four LH compartments. At least one compartment (#1) receives only uniglomerular input via the m-ACT, and one compartment (#3) does not receive m-ACT input at all. We were not able to clearly separate the innervation pattern of l-ACT and ml-ACT neurons due to methodological restrictions. Therefore, we do not know whether compartment #3 receives solely uPN input (via the l-ACT) or mixed input via uni- and multiglomerular PNs. Furthermore, the existence of c#4 still needs to be verified by selective labeling of ml-ACT1. In summary, our results show that the output from the AL is transferred to the LH via two uPN pathways (m- and l-ACT) and a mPN pathway (ml-ACTs). The different innervation patterns of the various ACTs suggest a differential processing of olfactory information in the LH. In vivo optical imaging in the LH after an anterograde fill of selected ACTs may further clarify this aspect in the near future.

Studies in *Drosophila* revealed a compartmentalization of the PN input to the LH neuropil. Marin et al. (2002) labeled two PN populations projecting via the inner ACT (the equivalent of the honeybee lateral ACT) branching across the entire LH. A third PN population projecting via the fly's medial ACT (an equivalent tract in the honeybee brain may be the ml-ACT2, see previous section) innervated only a small medioventral part of the LH. At the level of individual I-ACT uPNs, Marin et al. (2002), Wong et al. (2002), and Tanaka et al. (2004) found that PNs with input from specific glomeruli have restricted stereotypic terminal fields in the LH. They suggested that the LH neuropil has some degree of a chemotopic organization reflecting the organization of the AL. Tanaka et al. (2004) defined three LH zones based on these stereotypic PN innervations and could show that the arborizations from many LH third-order neurons were restricted within these zones.

What could be the functional indications of the anatomical compartmentalization of AL input in the LH? In all insects studied so far the LH of the protocerebral lobe constitutes the second target neuropil for uPNs of the m-ACT and, in the honeybee, additionally of the l-ACT. In contrast to the MBs, the LH also receives massive olfactory input from all multiglomerular PNs via the ml-ACTs. Multiglomerular PNs receive input from few to many glomeruli. Due to their rather sparse dendritic innervation within glomeruli these neurons probably have a high activation threshold. Thus, mPNs and the LH might detect more global changes of the current AL network stage and thus process more global features in the odor flow (suggested by Ignell and Hansson, 2005). The MBs, on the other hand, may promote fine discrimination of odor bouquets and their association with previous events (Heisenberg, 2003). Theories about the different function of MB and LH should also take into account that multimodal sensory integration within the LH represents a common and thus ancient feature of all insects studied so far, whereas the insect MBs have their evolutionary origin as purely olfactory neuropils (Gronenberg, 2001; Farris and Strausfeld, 2003; Schröter and Menzel, 2003). Finally, future studies of third-order interneurons with dendritic fields in the LH are needed to further clarify the function of LH subdivisions in the honeybee.

ml-ACTs and lateral network

From the three ml-ACTs in the honeybee brain the most caudal and ventral ml-ACT1 differ from the two others in that mPNs have no side branches along their way toward their target neuropil in the medial part of the LH. In contrast to this, mPNs of the ml-ACT 2 and 3 extend many side branches toward the rostral LPL on their way toward the LH.

We present a first anatomical characterization of the "lateral network" that is formed by the side branches and terminal arborizations of the mPN of the ml-ACT 2 and 3. Three distinct areas with dense olfactory innervation were identified: the ring neuropil, triangle, and lateral bridge. This anatomical characterization can be used to analyze the anatomy of individual protocerebral third-order interneurons and associate their arborizations to olfactory output regions within the LPL. For example, Rybak and Menzel (1993) showed that the lateral bridge is connected with the α-lobe via the α-LPL tract.

We presented one example of a single, possibly recurrent neuron, which we termed the ALF-1 neuron innervating the ring neuropil and triangle as well as the MB neuropil. Its soma lies close to the vertical lobe, and the dense processes with blebby endings are suggestive of efferent processes across the entire AL, some of which reach into the base of glomeruli. Neurons with a similar morphology are known from many insect species and were termed centrifugal neurons (reviewed by Anton and Homberg, 1999; Hansson and Anton, 2000; Gebhardt and Homberg, 2004; Ignell and Hansson, 2005). A neuron with a similar AL innervation pattern was also described in the honeybee and termed AL-1 neuron (Rybak and Menzel, 1993). The presumably afferent side branch of the ALF-1 neuron into the region of the lip-stratum of the MB's vertical lobe as well as the processes projecting in the distal peduncle might provide a feedback circuit from the MB neuropil to the AL. This is supported by the blebby nature of many fine (presumably axonal) branches in the AL. The ALF-1 shown here is likely similar to the partly filled neurons previously shown by Rybak and Menzel (1993) and Iwama and Shibuya (1998). The characteristic course of the axon around the vertical lobe and its large soma may allow future selected intracellular recordings,

TABLE 2. ACTs in Insect Species Investigated So Far and Their Proposed Relatedness

Reference	Species	Order	Inner ACT	Transversal ACTs (homologies uncertain)			Laterall-ACT
This study	***Apis melifera***	**Hymenoptera: Aculeata**		Mediolateral ACT 1 = ml-ACT1	Mediolateral ACT 2 = ml-ACT2	Mediolateral ACT 3 = ml-ACT3	Found only in these 3 species, likely homolog
Unpublished results	*Camponotus floridanus*	Hymenoptera: Aculeata					
	Paravespula germanica	Hymenoptera: Aculeata					
Homberg et al., 1988	*Manduca sexta*	Lepidoptera	Present;likely homologous	Dorsal ACT	Medial ACT, homolog in both species	Outer ACT, homolog in both species	—
Stocker et al., 1990	*Drosophila melanogaster*	Diptera		—			—
Wegerhoff, 1999; pers. commun.	*Tenebrio molitor*	Coleoptera		At least two transversal ACTs (unpublished results)			—
Malun et al., 1993	*Periplaneta americana*	Dictyoptera (superorder)		Three mediolateral ACTs		outer ACT	—
Unpublished results	*Forficula auricularia*	Dermaptera		Several mediolateral ACTs		outer ACT	—
Ignell, 2001	*Schistocerca gregaria*	Orthoptera		Dorsomedial ACT		outer ACT	—

For detailed definitions of the Inner ACT, Transversal ACT, and Lateral ACT, see text in the Discussion.

neurochemical characterizations, and further clarification of its function.

Considerations on the evolution of a dual uniglomerular olfactory pathway

To understand the evolution of the different ACTs in the hymenopteran brain, we need to determine both plesiomorphic (primitive) and derived features of the hymenopteran olfactory pathway. Findings of similar ACT anatomy and PN morphology in other insects would indicate a primitive trait. This applies to the m-ACT, which is probably homologous to the inner IACT in all insects studied so far (Table 2) (cf. review by Anton and Homberg, 1999). Unfortunately, for the other ACTs it is less clear which ones are homologous to each other in the various insect groups.

The closest hymenopteran relatives among studied holometabolous species belong to Diptera and Lepidoptera. They all share two additional "transversal ACTs," termed medial MACT and outer OACT. The existence of several ACTs that 1) are composed mainly of mPNs, 2) branch from or have a common route with the IACT, 3) project transversally across the protocerebrum, 4) send side branches into the LPL, 5) terminate in the LH, and 6) have no connection to the MBs is probably not only a common feature of Diptera and Lepidoptera, but a primitive trait of all Holometabola; similar tracts can be found in Coleoptera and in various hemimetabolous orders (Table 2). If we now search for ACTs in the *Apis* brain that share those six features, we find that the mediolateral ACTs 2 and 3 are the most likely ones to be homologous to the medial ACT and outer ACT in the species mentioned above. In other words, we assume that the ml-ACT 2 and 3 are plesiomorphic (primitive) features of the Hymenopteran brain. The ml-ACT 1 of the *Apis* brain shares five out of these six features, as it is lacking side branches innervating the LPL on its course toward the LH. So far, a nonbranching transversal ACT that innervates the LH has been described only in *Manduca sexta*: the dorsal ACT (Homberg et al., 1989).

What distinguishes the *Apis* olfactory pathway from that of the other insects studied so far is the existence of a prominent l-ACT, as second or additional, mainly uniglomerular, ACT that exits the dorsal AL, projects laterally to send side branches toward the LH, and to finally terminate in the duplicated calyces of the ipsilateral MB. So far, it has been assumed that the hymenopteran l-ACT is homologous to the OACT in *Drosophila* and *Manduca* (Anton and Homberg, 1999; Hansson and Anton, 2000). Two findings suggest the OACT as the precursor for the hymenopteran l-ACT: First, Abel et al. (2001) found in *Apis* a single multiglomerular PN that projected along the l-ACT and had only terminals in the LPL and none in the MB. Second, Homberg et al. (1988) described a rare type of uPN in *Manduca sexta* that projects through the OACT to innervate the LH and beyond to terminate in the MB calyx (called POd neurons). In *Drosophila,* as well, occasionally PNs can be found in the outer tract that project beyond the LH to the MB calyx (Ito, pers. commun.). However, our findings indicate that the ml-ACT 3 of Hymenoptera is the homolog to the outer ACT of others insects and that the l-ACT in its unique anatomy may be a derived feature of the honeybee olfactory system.

A prominent l-ACT with PNs projecting to the LH and MBs has been found only in the three aculeate species studied so far, but not in the other insect species. Based on currently accepted hypotheses of the phylogeny of Holometabola (Engel and Grimaldi, 2005), we can therefore assume that the l-ACT evolved sometime after the split of the ancestors of Hymenoptera and Panorpida (Lepidoptera, Diptera, and other orders) and before the differentiation of Aculeata (Vespoidea and Apoidea). Whether it emerged by graduated proliferation and specialization of OACT neurons or perhaps by a sudden duplication of whole parts of the olfactory system (IACT plus AL and calyx) remains an open question. To answer this, morphological studies in search of a dual olfactory pathway in non-aculeate hymenopteran species are needed.

ACKNOWLEDGMENTS

We thank Wulfila Gronenberg for help with neuroanatomical labeling techniques, Malu Obermayer for expert technical assistance, Susanne Schulmeister for valuable input on hymenopteran phylogeny, Dirk Ahrens for beekeeping and bee supply, and Sabine Krofczik and Vincent Dercksen for data transfer to the Honeybee Standard Brain website and help with the 3D data registration.

LITERATURE CITED

Abel R, Rybak J, Menzel R. 2001. Structure and response patterns of olfactory interneurons in the honeybee, *Apis mellifera*. J Comp Neurol 437:363–383.

Anton S, Homberg U. 1999. Antennal lobe structures. In: Hansson BS, editor. Insect olfaction. Heidelberg: Springer. p 97–124.

Anton S, van Loon JJA, Meijerink J, Smid HM, Takken W, Rospars J-P. 2003. Central projections of olfactory receptor neurons from single antennal and palpal sensilla in mosquitoes. Arthropod Struct Dev 32:319.

Arnold G, Masson C, Budharugsa S. 1985. Comparative study of the antennal lobes and their afferent pathways in the worker bee and the drone (*Apis mellifera*). Cell Tissue Res 242:593–605.

Bicker G, Kreissl S, Hofbauer A. 1993. Monoclonal-antibody labels olfactory and visual pathways in *Drosophila* and *Apis* brains. J Comp Neurol 335:413–424.

Brandt R, Rohlfing T, Rybak J, Krofczik S, Maye A, Westerhoff M, Hege HC, Menzel R. 2005. Three-dimensional average-shape atlas of the honeybee brain and its applications. J Comp Neurol 492:1–19.

Carlsson MA, Galizia CG, Hansson BS. 2002. Spatial representation of odours in the antennal lobe of the moth *Spodoptera littoralis* (Lepidoptera : Noctuidae). Chem Senses 27:231–244.

Christensen TA, White J. 2000. Representation of olfactory information in the brain. In: Finger TE, Silver WL, Restrepo D, editors. The neurobiology of taste and smell, 2nd ed. New York: Wiley-Liss. p 201–232.

Engel MS, Grimaldi DA. 2005. Primitive new ants in cretaceous amber from Myanmar, New Jersey, and Canada (Hymenoptera : Formicidae). Am Mus Novit 3485:1–23.

Ernst KD, Boeckh J, Boeckh V. 1977. Neuroanatomical study on organization of central antennal pathways in insects. 2. Deutocerebral connections in *Locusta migratoria* and *Periplaneta americana*. Cell Tissue Res 176:285–308.

Fahrbach SE. 2006. Structure of the mushroom bodies of the insect brain. Annu Rev Entomol 51:209–232.

Farris SM, Strausfeld NJ. 2003. A unique mushroom body substructure common to basal cockroaches and to termites. J Comp Neurol 456:305–320.

Flanagan D, Mercer AR. 1989. An atlas and 3-D reconstruction of the antennal lobes in the worker honey bee, *Apis mellifera* (Hymenoptera, Apidae). Int J Insect Morphol Embryol 18:145–159.

Fonta C, Sun XJ, Masson C. 1993. Morphology and spatial-distribution of bee antennal lobe interneurons responsive to odors. Chem Senses 18: 101–119.

Frambach I, Rössler W, Winkler M, Schürmann FW. 2004. F-actin at identified synapses in the mushroom body neuropil of the insect brain. J Comp Neurol 475:303–314.

Galizia CG, Kimmerle B. 2004. Physiological and morphological characterization of honeybee olfactory neurons combining electrophysiology, calcium imaging and confocal microscopy. J Comp Physiol [A] 190:21–38.

Galizia CG, Menzel R. 2000. Odour perception in honeybees: coding information in glomerular patterns. Curr Opin Neurobiol 10:504–510.

Galizia CG, Sachse S, Rappert A, Menzel R. 1999a. The glomerular code for odor representation is species specific in the honeybee *Apis mellifera*. Nat Neurosci 2:473–478.

Galizia GC, McIlwrath SL, Menzel R. 1999b. A digital three-dimensional atlas of the honeybee antennal lobe based on optical sections acquired by confocal microscopy. Cell Tissue Res 295:383–394.

Gebhardt S, Homberg U. 2004. Immunocytochemistry of histamine in the brain of the locust *Schistocerca gregaria*. Cell Tissue Res 317:195.

Groh C, Tautz J, Rössler W. 2004. Synaptic organization in the adult honey bee brain is influenced by brood-temperature control during pupal development. Proc Natl Acad Sci U S A 101:4268–4273.

Groh C, Ahrens D, Rössler W. 2006. Environment- and age-dependent plasticity of synaptic complexes in the mushroom bodies of honeybee queens. Brain Behav Evol 68:1–14.

Gronenberg W. 2001. Subdivisions of hymenopteran mushroom body calyces by their afferent supply. J Comp Neurol 435:474–489.

Grünewald B. 2003. Differential expression of voltage-sensitive K+ and Ca2+ currents in neurons of the honeybee olfactory pathway. J Exp Biol 206:117–129.

Hansson BS, Anton S. 2000. Function and morphology of the antennal lobe: new developments. Annu Rev Entomol 45:203–231.

Hansson BS, Christensen TA. 1999. Functional characteristics of the antennal lobe. In: Hansson BS, editor. Insect olfaction. Heidelberg: Springer. p 125–161.

Heisenberg M. 2003. Mushroom body memoir: from maps to models. Nat Rev Neurosci 4:266.

Hildebrand JG, Shepherd GM. 1997. Mechanisms of olfactory discrimination: converging evidence for common principles across phyla. Annu Rev Neurosci 20:595–631.

Homberg U, Montague RA, Hildebrand JG. 1988. Anatomy of antennocerebral pathways in the brain of the sphinx moth *Manduca sexta*. Cell Tissue Res 254:255–281.

Homberg U, Christensen T, Hildebrand JG. 1989. Structure and function of the deuterocerebrum in insects. Annu Rev Entomol 34:477–501.

Ignell R. 2001. Monoamines and neuropeptides in antennal lobe interneurons of the desert locust, *Schistocerca gregaria*: an immunocytochemical study. Cell Tissue Res 306:143–156.

Ignell R, Hansson BS. 2005. Projection patterns of gustatory neurons in the suboesophageal ganglion and tritocerebrum of mosquitoes. J Comp Neurol 492:214–233.

Ignell R, Anton S, Hansson BS. 2000. The maxillary palp sensory pathway of Orthoptera. Arthropod Struct Dev 29:295.

Itoh T, Yokohari F, Tominaga Y. 1991. Response to humidity change of deutocerebral interneurons of the honeybee, *Apis mellifera* L. Naturwissenschaften 78:320–322.

Iwama A, Shibuya T. 1998. Physiology and morphology of olfactory neurons associating with the protocerebral lobe of the honeybee brain. J Insect Physiol 44:1191–1204.

Joerges J, Küttner A, Galizia GC, Menzel R. 1997. Representation of odours and odour mixtures visualized in the honeybee brain. Nature 387:285–288.

Kelber C, Rössler W, Kleineidam CJ. 2006. Multiple olfactory receptor neurons and their axonal projections in the antennal lobe of the honeybee *Apis mellifera*. J Comp Neurol 496:395–405.

Kent KS, Oland LA, Hildebrand JG. 1999. Development of the labial pit organ glomerulus in the antennal lobe of the moth *Manduca sexta*: the role of afferent projections in the formation of identifiable olfactory glomeruli. J Neurobiol 40:28–44.

Klagges BRE, Heimbeck G, Godenschwege TA, Hofbauer A, Pflugfelder GO, Reifegerste R, Reisch D, Schaupp M, Buchner S, Buchner E. 1996. Invertebrate synapsins: a single gene codes for several isoforms in *Drosophila*. J Neurosci 16:3154–3165.

Kreissl S, Bicker G. 1989. Histochemistry of acetylcholinesterase and immunohistochemistry of an acetylcholine receptor-like antigen in the brain of the honeybee. J Comp Neurol 286:71–84.

Malun D, Waldow U, Kraus D, Boeckh J. 1993. Connections between the deutocerebrum and the protocerebrum, and neuroanatomy of several classes of deutocerebral projection neurons in the brain of male periplaneta-americana. J Comp Neurol 329:143–162.

Marin EC, Jefferis G, Komiyama T, Zhu HT, Luo LQ. 2002. Representation of the glomerular olfactory map in the *Drosophila* brain. Cell 109:243–255.

Menzel R. 2001. Searching for the memory trace in a mini-brain, the honeybee. Learn Mem 8:53–62.

Menzel R, Manz G. 2005. Neural plasticity of mushroom body-extrinsic neurons in the honeybee brain. J Exp Biol 208:4317–4332.

Mobbs PG. 1982. The brain of the honeybee *Apis mellifera*. 1. The connections and spatial-organization of the mushroom bodies. Philos R Soc Lond B 298:309–354.

Müller D, Abel R, Brandt R, Zockler M, Menzel R. 2002. Differential parallel processing of olfactory information in the honeybee, *Apis mellifera* L. J Comp Physiol [A] 188:359–370.

Nishikawa M, Yokohari F, Ishibashi T. 1995. Central projections of the antennal cold receptor neurons and hygroreceptor neurons of the cockroach *Periplaneta americana*. J Comp Neurol 361:165–176.

Nishino H, Yamashita S, Yamazaki Y, Nishikawa M, Yokohari F, Mizunami M. 2003. Projection neurons originating from thermo- and hygrosensory glomeruli in the antennal lobe of the cockroach. J Comp Neurol 455:40–55.

Pareto A. 1972. Spatial-distribution of sensory antennal fibers in central nervous-system of worker bees. Z Zellforsch Mikrosk Anat 131:109.

Rospars JP, Hildebrand JG. 1992. Anatomical identification of glomeruli in the antennal lobes of the male sphinx moth *Manduca sexta*. Cell Tissue Res 270:205–227.

Rössler W, Randolph PW, Tolbert LP, Hildebrand JG. 1999. Axons of olfactory receptor cells of transsexually grafted antennae induce devel-

opment of sexually dimorphic glomeruli in *Manduca sexta*. J Neurobiol 38:521–541.

Rybak J, Menzel R. 1993. Anatomy of the mushroom bodies in the honeybee brain — the neuronal connections of the alpha-lobe. J Comp Neurol 334:444–465.

Sachse S, Galizia CG. 2002. Role of inhibition for temporal and spatial odor representation in olfactory output neurons: a calcium imaging study. J Neurophysiol 87:1106–1117.

Sachse S, Galizia CG. 2003. The coding of odour-intensity in the honeybee antennal lobe: local computation optimizes odour representation. Eur J Neurosci 18:2119–2132.

Schäfer S, Bicker G. 1986. Distribution of GABA-like immunoreactivity in the brain of the honeybee. J Comp Neurol 246:287–300.

Schneider D, Steinbrecht A. 1968. Checklist of insect olfactory sensilla. Symp Zool Soc Lond 23:279–297.

Schröter U, Menzel R. 2003. A new ascending sensory tract to the calyces of the honeybee mushroom body, the subesophageal-calycal tract. J Comp Neurol 465:168–178.

Stocker RF, Lienhard MC, Borst A, Fischbach KF. 1990. Neuronal architecture of the antennal lobe in *Drosophila melanogaster*. Cell Tissue Res 262:9–34.

Strausfeld NJ. 2002. Organization of the honey bee mushroom body: representation of the calyx within the vertical and gamma lobes. J Comp Neurol 450:4–33.

Strausfeld NJ, Hildebrand JG. 1999. Olfactory systems: common design, uncommon origins? Curr Opin Neurobiol 9:634–639.

Suzuki H. 1975. Antennal movements induced by odour and central projection of the antennal neurones in the honeybee. J Insect Physiol 21:831–847.

Tanaka NK, Awasaki T, Shimada T, Ito K. 2004. Integration of chemosensory pathways in the *Drosophila* second-order olfactory centers. Curr Biol 14:449–457.

Vosshall LB, Wong AM, Axel R. 2000. An olfactory sensory map in the fly brain. Cell 102:147–159.

Wang JW, Wong AM, Flores J, Vosshall LB, Axel R. 2003. Two-photon calcium imaging reveals an odor-evoked map of activity in the fly brain. Cell 112:271–282.

Wegerhoff R. 1999. GABA and serotonin immunoreactivity during postembryonic brain development in the beetle Tenebrio molitor. Microscopy Research and Technique 45:154–164.

Wong AM, Wang JW, Axel R. 2002. Spatial representation of the glomerular map in the Drosophila protocerebrum. Cell 109:229–241.

Xu FQ, Greer CA, Shepherd GM. 2000. Odor maps in the olfactory bulb. J Comp Neurol 422:489–495.